An 800-kyr planktonic $\delta^{18}O$ stack for the ~~West~~ Western Pacific Warm Pool

Christen L. Bowman[1], Devin S. Rand[1], Lorraine E. Lisiecki[1], and Samantha C. Bova[2]
[1]Department of Earth Science, University of California Santa Barbara, Santa Barbara, CA, 93106, USA
[2]Department of Geological Sciences, San Diego State University, San Diego, CA, 92182, USA
Correspondence to: Lorraine E. Lisiecki (lisiecki@geol.ucsb.edu)

Abstract. The ~~West Pacific~~Western Pacific Warm Pool (WPWP) exhibits different glacial-interglacial climate variability compared to~~than~~ high latitudes, and its sea surface temperatures are thought to respond primarily to changes in greenhouse ~~gas~~forcing. To better characterize the orbital-~~-~~scale climate response covering the~~of the~~ WPWP, we constructed a planktonic $\delta^{18}O$ stack (average) of 10~~1~~ previously published WPWP records of the last 800 ka~~yr~~, available at https://doi.org/10.5281/zenodo.10211900 ~~https://doi.org/10.5281/zenodo.8190829~~ (Bowman et al., 2023), using new Bayesian alignment and stacking software BIGMACS (Lee and Rand et al., 2023). Similarities in stack uncertainty between the WPWP planktonic $\delta^{18}O$ stack and benthic $\delta^{18}O$ stacks, also constructed using BIGMACS, demonstrate that the software performs similarly well when aligning regional planktonic or benthic $\delta^{18}O$ data. Sixty-five~~seven~~ radiocarbon dates from the upper portion of five~~our~~ of the WPWP cores suggest that WPWP planktonic $\delta^{18}O$ change is nearly synchronous with global benthic $\delta^{18}O$ during the last glacial termination. However, the WPWP planktonic $\delta^{18}O$ stack exhibits a smaller~~less~~ glacial/interglacial amplitude and less spectral power at all orbital frequencies than benthic $\delta^{18}O$. We assert that the WPWP planktonic $\delta^{18}O$ stack provides a useful representation of orbital-scale regional climate response and a valuable regional alignment target, particularly ~~for~~ over the ~~higher resolution~~ 0 to~~-~~ 450 ka portion of ~~our~~ the stack.

1 Introduction

The tropical Pacific is an important source of heat and moisture to the atmosphere (e.g., De Deckker, 2016; Neale and Slingo, 2003; Mayer et al., 2014) and is thought to have a strong impact on global climate responses during glacial cycles (Lea et al., 2000). Prior studies suggest that the climate of the ~~West~~ Western Pacific Warm Pool (WPWP), which is defined by mean annual sea surface temperatures (SST) above 28°C, responds primarily to changes in greenhouse gas concentrations due to the region's large distance from high-latitude ice sheets (Broccoli et al., 2000; Lea, 2004; Tachikawa et al., 2014). Additionally, Earth's orbital cycles cause seasonal variations in insolation ~~(i.e., or~~ incoming solar radiation~~)~~, which affect Earth's high and low latitudes differently. In the WPW~~P~~W~~.~~, ~~with~~ only 0.3°C of ~~WPWP~~ SST change is attributed to orbital forcing during the Late Pleistocene (Tachikawa et al., 2014). Thus, climate records of the WPWP region are expected to have features which differ from the high-latitude climate records often used to ~~characterize~~describe global climate change (e.g., Lisiecki & Raymo, 2005; Past Interglacials Working Group of P~~ages~~AGES, 2016), ~~which differ from many other locations on Earth.~~ Here we seek to characterize WPWP climate on orbital timescales and its differences from high-latitude climate, which can help test hypotheses about the sensitivity of the WPWP to orbital forcing, ice volume, and greenhouse gas concentration.

One of the most commonly used paleoceanographic climate proxies is the ratio of oxygen isotopes, denoted as $\delta^{18}O$, in calcium carbonate from foraminiferal tests~~shells~~; this proxy is affected by both water temperature and the $\delta^{18}O$ of seawater, which varies with global ice volume as well as local salinity (Wefer and Berger, 1991). The two general types of foraminifera are benthic and planktonic, which live in the deep ocean and surface ocean, respectively. Benthic $\delta^{18}O$ is considered a high-latitude climate proxy because deep water temperature is set in high-latitude deep water formation regions and because global ice volume responds primarily to high-latitude northern hemisphere summer insolation. However, planktonic $\delta^{18}O$ is influenced by both high-latitude ice volume and local SST and salinity (Rosenthal et al., 2003). Previous studies from the WPWP have shown smaller glacial-interglacial amplitudes of planktonic $\delta^{18}O$ change than in benthic $\delta^{18}O$

Formatted: Font: 10 pt
Formatted: Font: 10 pt, Font color: Text 1
Formatted: Font: 10 pt, Font color: Text 1
Formatted: Font: 10 pt
Formatted: Font: 10 pt, Font color: Text 1
Formatted: Font: 10 pt, Font color: Text 1
Formatted: Font: 10 pt
Formatted: Font: 10 pt
Formatted: Font: 10 pt
Formatted: Font: 10 pt
Formatted: Font: 10 pt
Formatted: Font: 10 pt
Formatted: Font color: Text 1
Formatted: Font: 10 pt
Formatted: Font: 10 pt
Formatted: Font: 10 pt
Formatted: Font color: Text 1
Formatted: Font: 10 pt, Font color: Text 1
Formatted: Font color: Text 1
Formatted: Font: 10 pt, Font color: Text 1
Formatted: Font color: Text 1
Formatted: Font: 10 pt

or planktonic $\delta^{18}O$ from other regions (Lea et al., 2000; de Garidel-Thoron et al., 2005). This difference has been attributed to smaller sea surface temperature fluctuations and salinity changes in the WPWP (Broccoli et al., 2000; Lea et al., 2000; de Garidel-Thoron et al., 2005).

Here we present a stack (time-dependent average) of planktonic $\delta^{18}O$ records from ~~eleven~~ ten cores across the WPWP to provide a record of its regional responses over the past 800 k~~a~~yr~~s~~, which can be compared to the high-latitude response of global and regional benthic $\delta^{18}O$ stacks.

The ~~new~~ WPWP planktonic $\delta^{18}O$ stack ~~of the WPWP region presented here~~ is intended to better characterize orbital responses in WPWP planktonic $\delta^{18}O$ and to improve age models for WPWP sediment cores. Age models for ocean sediment cores, which provide estimates of sediment age as a function of core depth, are commonly constructed by stratigraphic correlation (i.e., alignment) of an individual core's $\delta^{18}O$ record to a global $\delta^{18}O$ stack such as the LR04 or SPECMAP stacks (Linsley and Breymann, 1991; Lea et al, 2000; Chuang et al., 2018; Lisiecki and Raymo, 2005; Imbrie et al., 1984). A stack is the time-dependent average of data from multiple ocean sediment cores that share a common climatic signal, thus increasing the signal-to-noise ratio of the data. Traditionally, stacks have been constructed from global compilations of benthic $\delta^{18}O$ (Lisiecki and Raymo, 2005), planktonic ~~$\delta^{18}O$~~ ~~$\delta^{18}O$~~ (Shakun et al., 2015) or a combination of the two (Imbrie et al., 1984; Huybers and Wunsch, 2004). However, recent studies have advocated the development of regional stacks (Lisiecki and Stern, 2016; Lee and ~~Ran~~Rand~~d~~ et al., ~~accepted~~2023) to distinguish spatial differences in the timing and amplitude of $\delta^{18}O$ changes.

We constructed a WPWP planktonic $\delta^{18}O$ stack spanning 0 to ~~-~~800 ~~kyr~~ ka using new Bayesian alignment and stacking software, BIGMACS (Lee and Rand et al., ~~accepted~~2023). The new stack consists of previously published planktonic $\delta^{18}O$ data and 65 radiocarbon dates ranging from 1.5~~1~~ to 36.9 ka from ten cores within the WPWP~~eleven tropical Western Pacific cores and 657 radiocarbon dates between ranging from 1.510 to 36.943 kyr BP from fiveour of the cores~~. ~~Here w~~We present the new WPWP stack and a brief comparison of orbital power in the new stack compared to the LR04 global benthic $\delta^{18}O$ stack (Lisiecki and Raymo, 2005) and a recently published stack of ~~I~~WPWP~~r~~egegional~~ional~~ -SST (Jian et al., 2022). We also evaluate the relative timing of WPWP planktonic $\delta^{18}O$ change versus benthic $\delta^{18}O$ change during the last glacial termination ~~(T1)~~.

2 Study a~~A~~rea

The ~~West Pacific~~Western Pacific Warm Pool is a region of the equatorial Pacific with annual average SST between 28°C to 30°C (Tachikawa et al., 2014). It covers an area between approximately 15 degrees S to 15 degrees N and 115 to 160 degrees E (Locarnini et al., 2018)~~, with boundaries defined by mean annual SST of greater than 28°C (Tachikawa et al., 2014)~~. Synchronous change in $\delta^{18}O$ is assumed ~~for the cores that are stacked~~during the stacking procedure (Lee & Rand et al., 2023), so homogeneous conditions in the core locations are important for maintaining the accuracy of the stack. The largely homogeneous WPWP surface ocean makes it a suitable choice for stacking (Lea et al., 2000; Li et al., 2011).

Cores were ~~chosen~~selected for inclusion based on their location in or near the WPWP, ~~and with an age range of approximately 400 kyr or longer. However, our new stack~~ includinges ~~t~~two~~two~~ cores just beyond the boundary of the typically defined WPWP region. We choose to include these two cores (ODP-1143 and MD05-2930) because of their high resolution and/or an ~~records extend~~age range that covers the full length of the stack~~., and they~~The cores' locations exhibit oceanographic variability broadly comparable to that observed within the warm pool proper over the period of interest. Core ODP~~--~~1143 from the South China Sea, which lies just beyond the northwestern border of the modern WPWP, has an average annual temperature of ~28°C and receives northward flowing water from the WPWP during summer (Li et al., 2011). Core MD05-2930 is located along the southern limit of the WPWP in the Gulf of Papua; its SST is primarily controlled by the Australasian Monsoon, with modern SST fluctuating between 26°C to~~-~~ 29°C (Regoli et al., 2015). The slightly cooler sea surface temperatures of these two cores are expected to yield slightly more positive $\delta^{18}O$ values than other WPWP sites; these sites ~~and~~ may also be ~~affected by~~sensitive to orbital-scale changes in the WPWP extent.

Formatted: Font: 10 pt
Formatted: Font: 10 pt, Not Highlight
Formatted: Font: 10 pt
Formatted: Font: 10 pt
Formatted: Font color: Text 1
Formatted: Font: 10 pt
Formatted: Font: 10 pt, Not Highlight
Formatted: Font: 10 pt
Formatted: Font: 10 pt
Formatted: Font: 10 pt
Formatted: Font: 10 pt
Formatted: Font: 10 pt

~~In this study we~~ To ~~use an Indo-Pacific Warm Pool (IPWP) SST stack to represent~~evaluate the contribution of temperature to planktonic $\delta^{18}O_c$ change in the WPWP, we use an Indo-Pacific Warm Pool (IPWP) SST stack (Jian et al., 2022). The IPWP has significant overlap with the WPWP but additionally ~~covers a broader area than the WPWP~~includes a portion of the Indian Ocean; however, the cores ~~included~~ in the Jian et al. (2022) stack are predominantly from the WPWP. The~~re is also significant overlap between the~~ IPWP and WPWP~~, both of which~~ have ~~high~~a mean annual SST of 28 °C and 29 °C, respectively (Locarini et al., 2018).

Formatted: Font: 10 pt
Formatted: Font color: Text 1
Formatted: Font: 10 pt, Font color: Text 1
Formatted: Font: 10 pt, Font color: Text 1
Formatted: Font color: Text 1
Formatted: Font: 10 pt
Formatted: Font color: Text 1
Formatted: Font: 10 pt, Font color: Text 1
Formatted: Font color: Text 1
Formatted: Font: 10 pt, Font color: Text 1
Formatted: Font color: Text 1
Formatted: Font: 10 pt, Font color: Text 1
Formatted: Font: 10 pt, Font color: Text 1
Formatted: Font color: Text 1
Formatted: Font: 10 pt, Font color: Text 1
Formatted: Font: 10 pt, Font color: Text 1
Formatted: Font color: Text 1
Formatted: Font: 10 pt

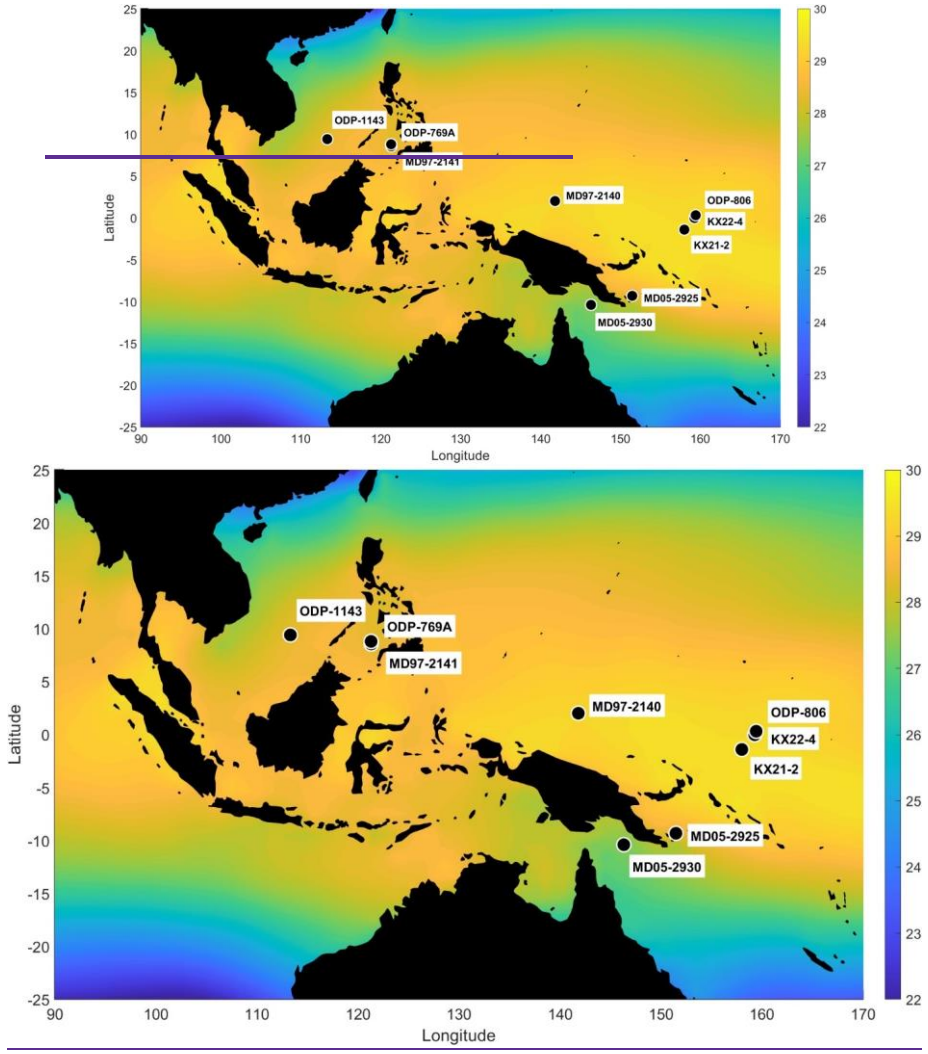

Figure 1. Core locations and mean annual sea surface temperatures (°C, color) from 1955-2018 (Locarnini et al., 2018). Created with MATLAB's geoshow() function from the mapping toolbox (The Mathworks Inc., R2023~~2a~~b).

Formatted: Centered

Formatted: Font: Not Bold

Formatted: Font color: Text 1

Formatted: Font: 9 pt, Font color: Text 1

Formatted: Font: 9 pt, Font color: Text 1

Formatted: Font color: Text 1

Formatted: Font color: Text 1

3 Data

We compiled ~~from the scientific literature~~previously published planktonic $\delta^{18}O$ measurements ~~of planktonic foraminifera~~ from ten~~eleven~~ tropical Western Pacific cores in or near the WPWP (**Table 1**). Cores were included in the stack based on their location in the WPWP, an age range spanning at least three glacial cycles, and an average time resolution of at least 4 kyr. ~~Six~~ Four~~of the~~ cores span the last ~~extend back to~~ 350~~0~~ to ~~-~~500 ka, and ~~five~~ six ~~span the last~~extend back to at least 750 ~~kyr~~ ka (**Fig. 2**). ~~-~~All but one core in the stack uses $\delta^{18}O$ values measured from the planktonic species *Globigerinoides ruber (G. ruber)* sensu stricto (s.s.), whose depth habitat in the WPWP ranges from the upper 45 m to ~~upper s~~105 m of the mixed layer depending on how calcification depth is calculated (Hollstein et al., 2017). ~~whose depth habitat is the upper 30m of the mixed layer (Wang, 2000).~~ One core, ODP ~~180~~ 1115B, has data from a different planktonic species, *Trilobatus sacculifer* (formerly ~~-~~*Globigerinoides sacculifer* ~~(G. sacculifer)~~, whose depth habitat is 20 m to 75 m or potentially as deep as 45 m to 95 m (Sadekov et al., 2009; Hollstein et al., 2017). ~~whose depth habitat is 20–75m (Sadekov et al., 2009).~~ A species correction of -0.11‰ was applied to the *~~TG~~. sacculifer* data according to the values presented by Spero et al. (2003). The average mixed layer depth of the WPWP is 50 m to 100 m (Locarini et al., 2018).~~-~~

A total of ~~,~~476~~25569~~ planktonic $\delta^{18}O$ measurements were used to create the stack. The stack spans from 0 to~~-~~ 800 ka; however, there is a significant decrease in data density ~~from~~ at 450~~ to ~~800~~~~ ka. Only six~~five~~ cores extend beyond 450 ka, and this portion of the stack is composed of only 960~~833~~ data points. The lower data resolution results in greater uncertainty and smoothness for the $\delta^{18}O$ features in the older portion of the stack; therefore, we focus our analysis of the stack ~~on the first~~upon the 0 to 450 ka portion~~yr~~.

The stacking algorithm counts each $\delta^{18}O$ measurement equally, so cores with higher resolution have more influence on the stack. The mean sample spacing ~~of the core data~~in the core records used to create the stack ranges from 0.55~~33~~ to ~~-~~3.9 kyr, with lower average sample spacing for the long cores that extend to the older half of the stack. Published data for core MD97-2141 has an average sedimentation rate of 5-15 cm/yr and is sampled at 1 cm intervals with a mean sample spacing of 0.11 kyr (Oppo et al., 2003). However, we smoothed the data using a 5-point running mean sampled ~~at~~ every fifth point, which reduces its mean sample spacing to 0.55 kyr, so that this one record does not overly dominate the regional stack. ~~Although the published data for core MD97-2141 has a mean sample spacing of 0.11 kyr, we smoothed the data using a 3-point running mean and reduced its mean sample spacing to 0.33 kyr, so that it does not overly dominate the regional stack.~~ Additionally, we constrain the stack age model using 6~~57~~ previously published radiocarbon measurements ranging from 1.52~~0.89~~ ka to 36~~43~~,9~~46~~ ka from five~~our~~ cores (Oppo et al., 2003;~~Holbourn et al., 2005; Jian et al., 2022;~~ Regoli et al., 2015; Lo et al., 2017, Dang et al., 2020, Zhang et al., 2021~~; Regoli et al., 2015~~).

Table 1. Locations of cores in the WPWP stack and the temporal coverage of their planktonic $\delta^{18}O$ data.

Core	Latitude	Longitude	Oldest Age (ka)	Avg Resolution (kyr)	Original Publication
~~ODP806~~	~~0.30~~	~~159.40~~	~~469.1~~	~~2.30~~	~~Lea et al., 2000~~
~~ODP124-769A~~	~~8.79~~	~~121.29~~	~~774.1~~	~~1.22~~	~~Linsley and Breymann, 1991~~
ODP 1143	9.40	113.30	798.3	1.83	Tian~~Li~~ et al., 2006~~2011~~
ODP 769A~~180-1115B~~	~~8.79-9.19~~	121.29~~151.57~~	774.1~~798.7~~	1.22~~.24~~	Linsley and Breymann, 1991~~Chuang et al., 2018~~
MD97-2141[a]	8.80	121.30	395.6	0.55~~33~~[b]	Oppo et al., 2003
MD97-2140	2.00	141.80	797.2	3.90	de Garidel-Thoron et al., 2005
MD05-2930 [a]	-10.42	146.30	799.7	2.03	Regoli et al., 2015
MD05-2925 [a]	-9.34	151.46	462.7	0.76	Lo et al., 2017; Lo, 2021
ODP 1115B	-9.19	151.57	798.7	2.24	Chuang et al., 2018
KX21-2 [a]	-1.42	157.98	394.5	0.93	Dang et al., 2020
KX22-4 [a]	-0.028	159.25	357.7	0.57	Zhang et al., 2021
ODP 806	0.30	159.40	800.5	2.27	Lea et al., 2000; Medina-Elizalde and Lea, 2005

Formatted ...
Formatted ...
Formatted ...
Formatted ...
Formatted ...
Formatted ...
Formatted ...
Formatted ...
Formatted ...
Formatted ...
Formatted ...
Formatted ...
Formatted ...
Formatted ...
Formatted ...
Formatted ...
Formatted ...
Formatted ...
Formatted ...
Formatted ...
Formatted ...
Formatted ...
Formatted ...
Formatted ...
Formatted ...
Formatted ...
Formatted ...
Formatted ...
Formatted ...
Formatted ...
Formatted ...
Formatted ...
Formatted ...
Formatted ...
Formatted ...
Formatted ...
Formatted ...
Formatted ...
Formatted ...
Formatted ...
Formatted ...
Formatted ...
Formatted ...
Formatted ...
Formatted ...
Formatted ...
Formatted ...

MD01-2378 [a]	-13.08	121.79	459.6	1.08	Holbourn et al., 2005
SO18480-3 [a]	-12.09	121.65	307.0	0.43	Jian et al., 2022

[a] -indicates core with radiocarbon data, [b] indicates new resolution after smoothing and subsampling

Formatted: Font: 9 pt

Formatted: Space After: 0 pt

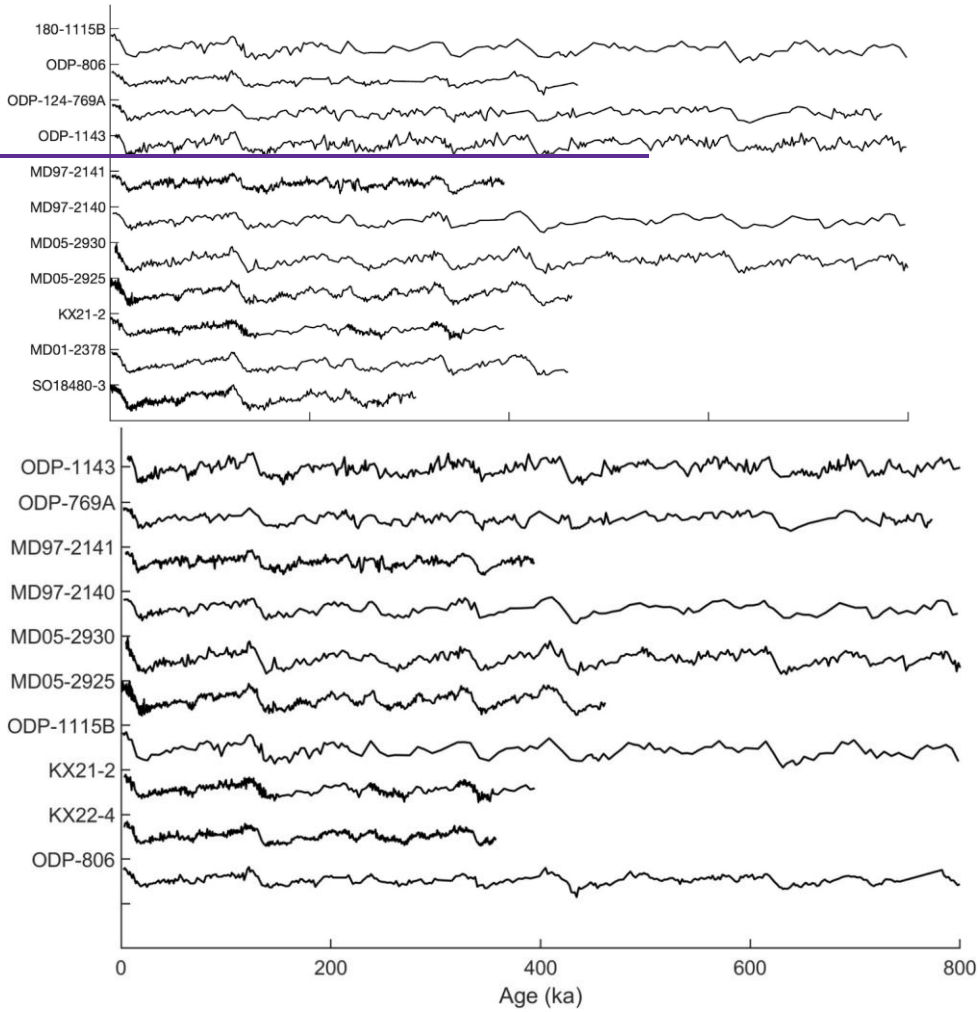

Figure 2. Planktonic $\delta^{18}O$ data of the cores used in the WPWP stack ~~construction~~, plotted on BIGMACS age models for each core and offset vertically. Data are from sites ODP-1143 (Tian et al., 2006), ~~180-1115B (Chuang et al., 2018),ODP-806 (Lea et al., 2000),~~ ODP ~~-124-~~769A (Linsley and Breymann, 1991), ~~ODP-1143 (Li et al., 2011),~~ MD97-2141 (Oppo et al., 2003), MD05-2140 (de Garidel-Thoron et al., 2005), MD05-2930 (Regoli et al., 2015), MD05-2925 (Lo et al., 2017; Lo, 2021), ODP-1115B (Chuang et al., 2018), KX21-

Formatted: Space Before: 18 pt

2 (Dang et al., 2020), KX22-4 (Zhang et al., 2021), ODP-806 (Lea et al., 2000; Medina-Elizalde and Lea, 2005)., MD01-2378 (Holbourn et al., 2005), and SO18480-3 (Jian et al., 2022).

4 Methods

4.1 Stack cConstruction

We use the new Bayesian software package BIGMACS to construct the planktonic $\delta^{18}O$ WPWP planktonic $\delta^{18}O$ stack (Lee and Rand et al., accepted2022023). BIGMACS, which stands for Bayesian Inference Gaussian process regression and Multiproxy Alignment for Continuous Stacks, constructs multiproxy age models and stacks by combining age information from both direct age constraints (e.g., radiocarbon data) and probabilistic alignments of $\delta^{18}O$ to a target record. Although BIGMACS was developed for benthic $\delta^{18}O$, here we use BIGMACS to align and stack planktonic $\delta^{18}O$; thus, we present analysis to verify the performance of the software for this new application.

BIGMACS stack construction is an iterative process with two steps. In the first step, age models are estimated for each record by aligning to an initial target. Each $\delta^{18}O$ record is shifted and scaled to better match the target stack during alignment, and likelihoods assigned to age estimates for each core depth are based on residuals between the core's shifted-and-scaled $\delta^{18}O$ value and the target's time-dependent mean. Likelihoods also depend on the target's and time-dependent and standard deviation. The shift/scale values represent how each core was adjusted to better match the alignment target. During alignment, shift and scale parameters are learned to correct for differences in species and latitudes. BIGMACS updates its alignment parameters using the Expectation Maximization (EM) algorithm to maximize likelihood. Core sites with homogeneous planktonic $\delta^{18}O$ values to have shift parameters close to 0 and scale parameters close to 1. In the second step, a stack is constructed with a Gaussian process regression over all $\delta^{18}O$ data using the aligned age models, and the stack's mean and amplitude are set to match the average values of the component records. The new stack is then used as the alignment target to construct age models for the next iteration, with alignment parameters updated to maximize likelihood using the Expectation Maximization (EM) algorithm. Iterations are performed until convergence. Core-specific shift and scale parameters (**Table 2**) reflect how much each individual record differs from the stack based on the assumption that all records share the same underlying signal but allowing for some scaling or offset based on consistent temperature/salinity gradients within the region as well as foraminiferal species differences (vital effects and depth habitat). Near-homogeneous planktonic $\delta^{18}O$ values between cores (and similar to the final stack) are indicated by shift parameters close to 0 and scale parameters close to 1. In the second step, a stack is constructed using the age models. The new stack is then used as the alignment target to construct age models for the next iteration. Iterations are performed until convergence.

The initial alignment target we used for constructing the WPWP stack was the LR04 stack of 57 globally distributed benthic $\delta^{18}O$ records (Lisiecki and Raymo, 2005) with a constant standard deviation of 0.5 ‰. The original age model for the LR04 stack was created by orbital tuning to a simple ice volume model and has estimated age uncertainties of +/- 4 kyr for the past 800 kyrka, i.e., time range of the WPWP stack (Lisiecki and Raymo, 2005). Despite the age uncertainty of the LR04 stack and the fact that it reflects benthic rather than planktonic $\delta^{18}O$, it was chosen as the initial alignment target because it is a widely used age model that spans the full 800 kyr time range of the new WPWP stack. Because the stack alignment target is shifted and scaled to match its component records during each iteration, the final stack output by BIGMACS reflects the average WPWP planktonic $\delta^{18}O$ values, rather than the benthic $\delta^{18}O$ values of the initial target.

Importantly, BIGMACS assumes that all records in the stack are homogeneous, i.e., that they all share the same underlying signal (with allowance for site-specific shift and scale values). Under this assumption, all residuals between individual $\delta^{18}O$ d18O measurements and the stack are assumed to reflect variability associated with sampling noise, measurement uncertainty and/or alignment uncertainty. Therefore, when stacking with BIGMACS, it is important to choose records for inclusion in the stack that share the same regional influence. Additionally, because all measurements are treated equally, cores with higher resolution data are more strongly weighted in the stack construction. The stack uncertainty reported by BIGMACS is the time-dependent standard deviation of a Gaussian fit to the $\delta^{18}O$ residuals. To evaluate whether the assumptions of homogeneity used by BIGMACS for stack construction areis applicable to the WPWP planktonic $\delta^{18}O$

Formatted: Font color: Text 1
Formatted: Font: 10 pt
Formatted: Font: 10 pt
Formatted: Font: 10 pt, Font color: Text 1
Formatted: Font: 10 pt
Formatted: Font: 10 pt
Formatted: Font: 10 pt
Formatted: Font: 10 pt
Formatted: Font: 10 pt, Bold
Formatted: Font: 10 pt
Formatted: Font: 10 pt
Formatted: Font: 10 pt

records in our new stack, Section 6.2 compares the WPWP planktonic stack uncertainty and the average alignment uncertainty of the stacked records to results from previously published regional benthic $\delta^{18}O$ stacks.

4.2 Stack age constraints

The first 3743 ka kyr Before Present (BP) of the WPWP are constrainedis constrained by 657 radiocarbon dates from fiveour cores. We calibrated radiocarbon ages using the Marine20 calibration curve (Heaton et al., 2020), which a reservoir age offset (ΔR) of 0 kyr, and reservoir age standard deviations of 0.2 kyr. The Marine20 calibration curve uses a model estimate of time-dependent global mean surface reservoir age, with values of, which is ~400 yr forin the Holocene and increases to 800 to 1000 yr fromor 20 to 50 kyr agoka (Heaton et al., 2020). We set the reservoir age offset (ΔR) for our sites to 0 yr, meaning we did not change the sites' reservoir ages from the time-dependent Marine20 default. We assigned a 1-sigma uncertainty of 200 yr to the reservoir ages to account for possible changes to the reservoir age offset of the WPWP relative to the Marine20 time-dependent global mean reservoir age. Ages for the remainder of the stack are largely determined by the timing of glacial cycles in the LR04 stack. Thus, the timing of planktonic $\delta^{18}O$ change in the WPWP stack is assumed to be synchronous with the LR04 benthic stack. In section 6.1, we show that there is strong agreement between in the timing of planktonic and benthic $\delta^{18}O$ change within WPWP cores and between in the WPWP stack and the LR04two benthic stacks during the firstfrom 1.50 to 3743 ka BP, in the interval for which WPWP ages are predominantly determined by radiocarbon data.

Core age models were also constrained by age estimates for the first and last $\delta^{18}O$ measurement from each core based on previous publications. Because these previous age estimates were based on a variety of age estimation methods, these previously published age Age uncertainty for these estimatesthey were assigned a Gaussian uncertainty distribution with a relatively large standard deviation of 4 kyr. Additionally,Lastly, we added tie points were included for two cores (ODP 180-1115B at 75 ka and, MD97-2141 at 63 ka and 92.5 ka) , and SO18480-3 at 75 ka to improve the alignment of Marine Isotope Stages (MIS) 3 and 4 to the target stack. Because tThese tie points were assigned based on direct identification of stratigraphic features in these two cores andcompared directly to the target stack, we assigned these tie point age estimates a smaller a Gaussian distribution with a standard deviation of 1 kyr. .

4.32 Conversions of SST and sea level to isotopic equivalents

We compare the amplitude of the new WPWP planktonic $\delta^{18}O$ stack with a sea level (ice volume) record and an IPWP SST stack, each of which is converted to the amount of planktonic $\delta^{18}O$ change they are expected to causeproduce. To compare the amplitude of WPWP planktonic $\delta^{18}O$ change with the ice volume (sea level) and WPWP SST changes that affect planktonic $\delta^{18}O$, we convert a sea level record and WPWP SST stack to the amount of $\delta^{18}O$ change they are expected to cause. The global sea level stack of Spratt and Lisiecki (2016) was used to calculate an equivalent change in seawater $\delta^{18}O$ due to ice volume ($\Delta\delta^{18}O_{ice}$) using a conversion of 0.009 ‰ per meter of sea level. This conversion represents the long-term average effect of ice volume change because the size of the effect varies slightly depending on the average $\delta^{18}O$ composition of the ice (Spratt and Lisiecki, 2016).

The IWPWP SST stack from Jian et al. (2022) was converted to an $\delta^{18}O$ equivalent using Eq. (1):

$$\Delta\delta^{18}O_{SST} = \frac{-1(SST-29)}{4.8} \quad (1)$$

The 4.8 scaling factor was presented byis taken from Bemis et al. (1998). A shift of 29 was chosen to express the effects of SST change relative to a modern WPWP mean SST of 29 °C. Thus, the resulting $\Delta\delta^{18}O_{SST}$ measures change relative to to World Ocean Atlas 2018 mean annual SST of the WPWP from 1955 - 2018 (Locarini et al., 2018), the present day.

4.43 Spectral aAnalysis

Power spectral density was calculated to quantify the strengths of response to orbital frequencies in $\delta^{18}O$ for our the WPWP and the LR04 stacks (Lisiecki and Raymo, 2005). TheBoth stacks were sub-sampled at 1 kyr spacing from 0 to 800 ka BP,

Formatted: Font: 10 pt, Bold
Formatted: Font: 10 pt
Formatted: Font: 10 pt, Font color: Text 1
Formatted: Font: 10 pt, Font color: Text 1
Formatted: Font: 10 pt, Font color: Text 1
Formatted: Font: 10 pt
Formatted: Font: 10 pt
Formatted: Font color: Text 1
Formatted: Font: (Default) +Body (Times New Roman), 10 pt, Font color: Text 1
Formatted: Font: 10 pt, Font color: Text 1
Formatted: Font: (Default) +Body (Times New Roman), 10 pt, Font color: Text 1
Formatted: Font: 10 pt, Font color: Text 1
Formatted: Font: (Default) +Body (Times New Roman), 10 pt, Font color: Text 1
Formatted: Font: 10 pt, Font color: Text 1
Formatted ...
Formatted: Font: 10 pt, Font color: Text 1
Formatted ...
Formatted: Font: 10 pt, Font color: Text 1
Formatted ...
Formatted: Font: 10 pt, Font color: Text 1
Formatted: Font: 10 pt
Formatted: Font: 10 pt
Formatted: Font: 10 pt, Font color: Text 1
Formatted: Font: 10 pt, Font color: Text 1
Formatted: Font: 10 pt, Font color: Text 1
Formatted: Font: 10 pt, Font color: Text 1
Formatted: Font: 10 pt, Font color: Text 1
Formatted: Font: 10 pt, Font color: Text 1
Formatted: Font: 10 pt, Font color: Text 1
Formatted: Font: 10 pt, Font color: Text 1
Formatted: Font: 10 pt, Font color: Text 1
Formatted: Font: 10 pt, Font color: Text 1
Formatted: Font: 10 pt
Formatted: Font: 10 pt, Font color: Text 1
Formatted: Font color: Text 1
Formatted: Font color: Text 1
Formatted: Font: 10 pt

and pPower spectral density was calculated from a Fast Fourier Transform (FFT) with the number of frequencies set to 1024using athe multitaper power spectral density estimate function pmtm( ) in MATLAB, with the number of tapers set to two, a rate of one sample per kyr, and an nfft of 512 (The MathWorks Inc., R2023a2b). Frequencies corresponding to the orbital cycle lengths of eccentricity (100 kyr), obliquity (41 kyr), and precession (23 and 19 kyr) are of particular interest to see how the insolation changes from the cycles affect the $\delta^{18}O$ values.

Normalized power spectral density was also calculated using the same method and sub-sampling for the IWPWP SST stack and our WPWP $\delta^{18}O$ stack from 0 to -360 ka to match the age range of the SST stack (Jian et al., 2022). The power spectral density of each record was normalized by dividing by the maximum peak height of the dominant ~100 kyr glacial cycle to evaluate the relative strength of different orbital frequencies.

5 Results

The probabilistic stack created by BIGMACS models the planktonic $\delta^{18}O$ value of the WPWP at any point in time as a Gaussian distribution with a time-varying mean and standard deviation. BIGMACS also estimates and applies shift and scale parameters for each core to optimize fit with the stack (**Table 2**). The standard deviation of the stack reflects scatter in the shifted-and-scaled $\delta^{18}O$ measurements at each point in time, including the effects of statistical uncertainty in each core's ~~$\delta^{18}O$ alignment to the stack~~age model. TThe standard deviation of the stack does not include any information about absolute age uncertainty (outside the range of radiocarbon). However, uncertainty does increase where data are ~~more~~ sparse. The standard deviation of the new WPWP planktonic $\delta^{18}O$ stack has an average value of 0.19 ~~20~~‰ for the full stack and 0.17 ~~8~~‰ for 0 to -450 ka, where data ~~coverage is~~are ~~most~~ more densely spaced.

Formatted: Font: 10 pt, Not Highlight
Formatted: Font: 10 pt, Not Highlight
Formatted: Font: 10 pt
Formatted: Font: 10 pt, Not Highlight
Formatted: Font: 10 pt
Formatted: Font: 10 pt, Not Highlight
Formatted: Font: 10 pt
Formatted: Font: 10 pt, Not Highlight
Formatted: Font: 10 pt
Formatted: Font: 10 pt, Not Highlight
Formatted: Font: 10 pt, Font color: Text 1
Formatted: Font: 10 pt, Not Highlight
Formatted: Font color: Text 1
Formatted: Font: 10 pt
Formatted: Font: 10 pt, Bold
Formatted: Font: 10 pt
Formatted: Font: 10 pt, Pattern: Clear
Formatted: Font: 10 pt
Formatted: Font: 10 pt
Formatted: Font: 10 pt, Pattern: Clear
Formatted: Font: 10 pt, Pattern: Clear
Formatted: Font: 10 pt

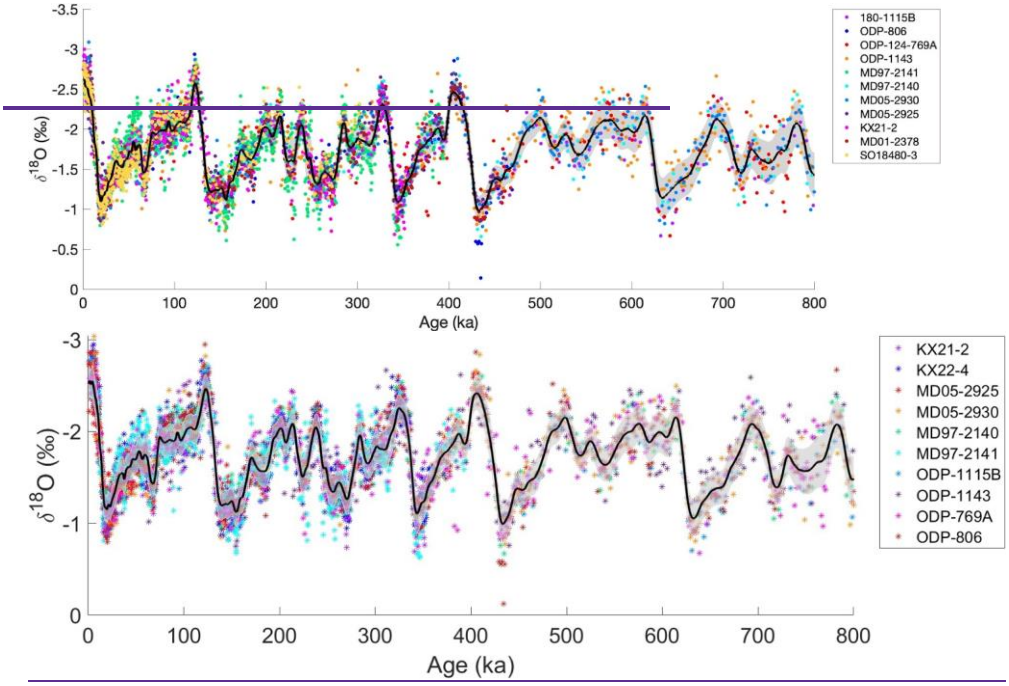

Figure 3. The WPWP planktonic δ^{18}O stack mean (black) and 1 standard deviation (gray shading). Colored asteriskdsots show the planktonic δ^{18}O measurements from each core after applying the core-specific shift and scale parameters calculated during alignment. Data from MD97-2141 was smoothed and sampled at one-fifththird the originally published resolution.

Table 2. Core-specific sShift and,t and scale parameters, and- the δ^{18}O residual standard deviation of δ^{18}O residuals values forbetween the WPWP stack and each core (after applying the estimated shift and scale parameters). in the WPWP stack.

Core	Shift	Scale	δ^{18}O Rresidual σtd (‰)
ODP 1143KX21-2	-0.38-0.26764	0.804831.09	0.23
ODP 769AODP-806	-0.53-0.33788	0.726190.81	0.72
MD97-2141 ODP-1143	-0.6244173	1.040.8	0.20
MD97-2140ODP-124-769A	-0.2354915	0.782910.92	0.17
MD05-2930MD97-2141	-0.6228900.46	0.77251.1	0.18
MD05-2925MD97-2140	-0.2695500.23	0.880781.11	0.15
ODP 1115BMD05-2930	0.640.46154	1.08641.14	0.17
KX21-2MD05-2925	-0.240.2283	1.086100.83	0.18
KX22-4180-1115B	-0.190.56016	1.07850.79	0.16
ODP 806MD01-2378	-0.350.03179	1.00360.72	0.18
SO18480-3	0.088366	1.0913	

Standard deviation of δ^{18}O residuals are calculated after each core is shifted and scaled

11

Formatted: Font: 10 pt
Formatted: Font: 10 pt, Not Bold
Formatted: Font: 10 pt, Not Bold
Formatted: Font: 10 pt, Not Bold
Formatted: Font: 10 pt, Not Bold
Formatted: Font: 10 pt
Formatted: Font: 10 pt
Formatted: Font: 10 pt
Formatted: Font: Symbol, 10 pt
Formatted: Font: 10 pt
Formatted: Font: 10 pt, Not Bold
Formatted: Font: 10 pt
Formatted: Font: 10 pt
Formatted: Font: 10 pt
Formatted: Font: 10 pt
Formatted: Font: 10 pt
Formatted: Font: 10 pt
Formatted: Font: 10 pt
Formatted: Font: 10 pt
Formatted: Font: 10 pt
Formatted: Font: 10 pt
Formatted: Font: 10 pt
Formatted: Font: 10 pt
Formatted: Font: 10 pt
Formatted: Font: 10 pt
Formatted: Font: 9 pt

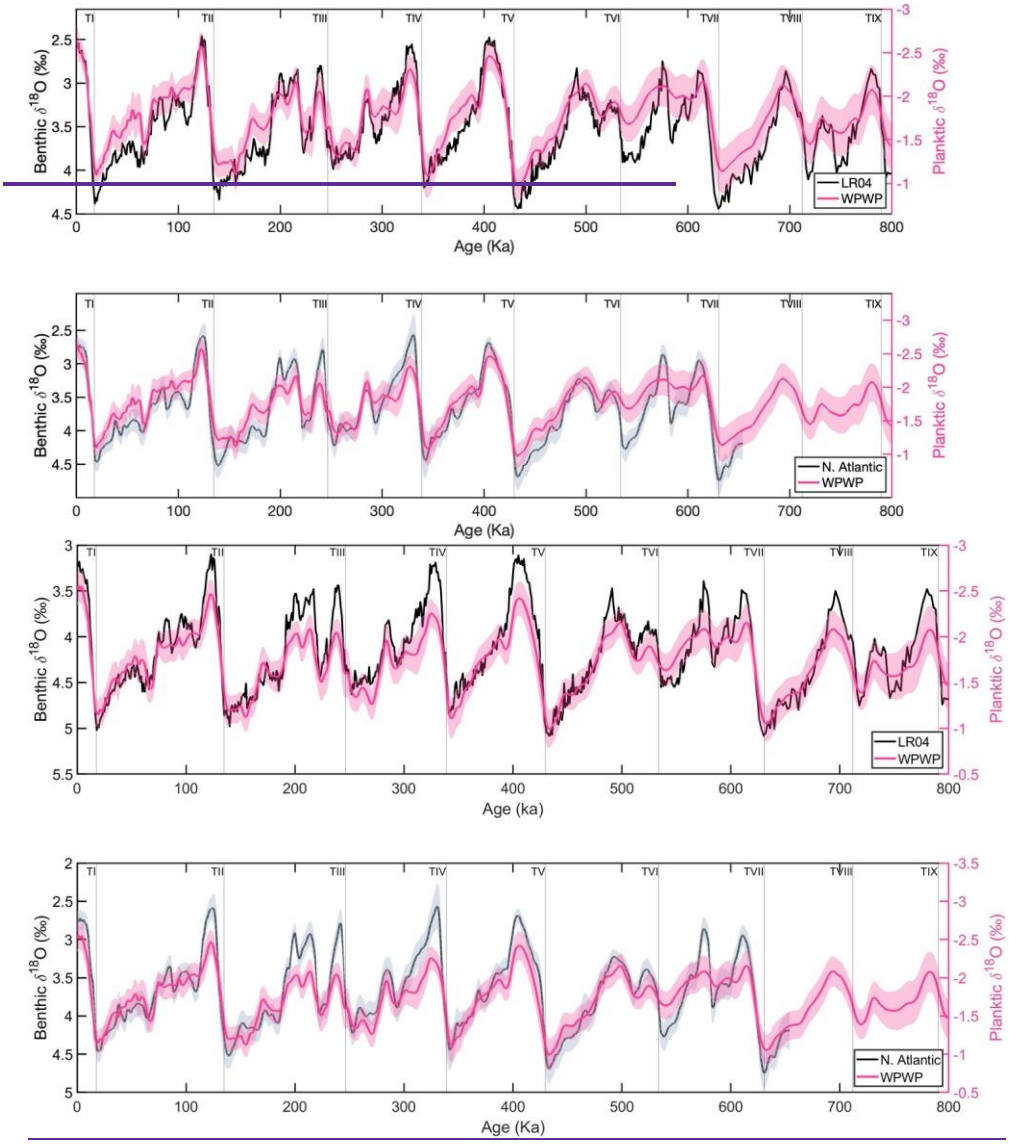
TI
TII
TIII
TIV
TV
TVI
TVII
TVIII
TIX
Benthic δ^{18}O (‰)
Planktic δ^{18}O (‰)
LR04
WPWP
Age (Ka)
N. Atlantic
WPWP
Age (Ka)
LR04
WPWP
Age (ka)
N. Atlantic
WPWP
Age (Ka)

Figure 4. Stack comparisons. (top) Comparison between our WPWP planktonic $\delta^{18}O$ stack (pink) and the global ~~benthic $\delta^{18}O$~~ LR04 benthic $\delta^{18}O$ stack (black) (Lisiecki and Raymo, 2005). (bottom) Comparison between our WPWP planktonic $\delta^{18}O$ ~~WPWP~~ stack (pink) and a regional North Atlantic benthic $\delta^{18}O$ stack (black) (Hobart et al., 2023). Shaded error bars represent one standard deviation in the WPWP and North Atlantic stacks. Glacial terminations are labelled with vertical lines based on ages for TI - TVII from Hobart et al. (2023); and TVIII-TIX from Lisiecki and Raymo (2005).

The ~~planktonic~~ WPWP planktonic stack has ~~a~~ weaker ~~the~~ glacial-interglacial amplitudes than the global LR04 benthic $\delta^{18}O$ stack (Lisiecki and Raymo, 2005) ~~and~~ or a North Atlantic benthic $\delta^{18}O$ stack produced by BIGMACS (Hobart et al., 2023)~~s~~. The average glacial~~/~~-interglacial amplitude for Terminations I to~~-~~ V is 1.7 ± 0.1 ‰ and 1.8 ± 0.1 ‰ in the LR04 and North Atlantic benthic stacks, respectively, but only 1.2 ± 0.1 ~~3~~‰ in the WPWP planktonic stack. (The reported o~~O~~ne standard deviation uncertainty for the mean amplitude of each stack~~s~~ is calculated using the time-dependent standard deviation of $\delta^{18}O$ in each stack.) This amplitude difference is also reflected in the spectral analysis of the stacks. Across all three orbital frequencies, there is greater spectral power in the ~~benthic~~ LR04 benthic stack than the ~~planktonic~~ WPWP planktonic stack (**Fig. 5**). ~~The total variance in the LR04 stack from 0–800 ka is 0.1256‰^{2} whereas the total WPWP variance is only 0.0694‰^{2}.~~

Formatted: Font: 10 pt
Formatted: Font: 10 pt
Formatted: Font: 10 pt
Formatted: Font: 10 pt
Formatted: Font: 10 pt
Formatted: Font: 10 pt

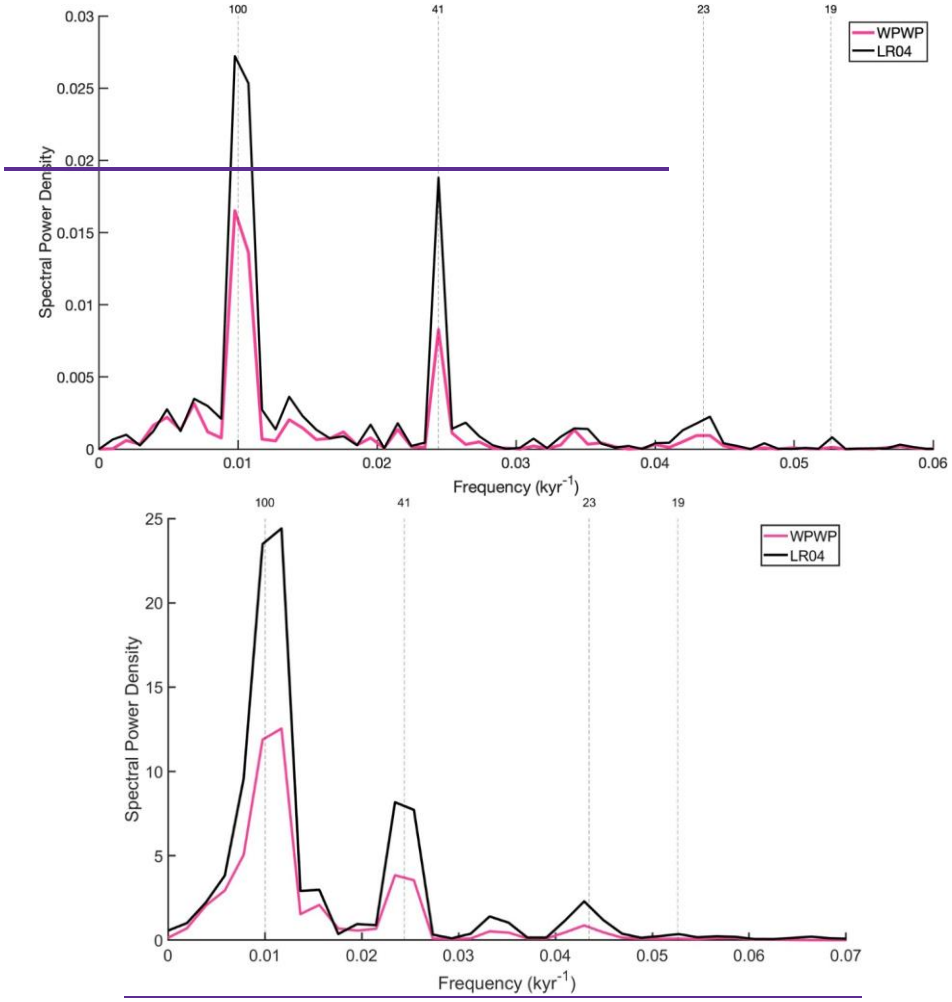

Figure 5. Spectral power density of ~~our~~ the WPWP planktonic $\delta^{18}O$ ~~WPWP~~ stack (pink) and the LR04 benthic $\delta^{18}O$ stack (black). Spectral power is calculated from 0 to ~~-~~800 ka for both stacks using MATLAB's p~~t~~mtm( ) function (The Mathworks Inc., R2023a~~2b~~). Orbital frequencies that correspond to 100, 41, 23 and 19 kyr are labeled with vertical dashed lines.

Formatted: Centered

Formatted: Font color: Text 1

Formatted: Font: 10 pt, Font color: Text 1

Formatted: Font color: Text 1

6 Methods validation and limitations

6.1 Age model assumptions

The use of the LR04 stack as an initial alignment target for our WPWP stack assumes benthic and planktonic $\delta^{18}O$ are changing synchronously; however, the signals recorded by benthic and planktonic $\delta^{18}O$ could differ in timing due to either a different transit time of the global ice volume signal to the deep ocean compared to surface of the WPWP tropical West Western Pacific and/or due to asynchronous temperature and salinity changes between the WPWP and high-latitude deep water formation regions. To evaluate potential timing differences in the two signals, we compare the age model for the portion of the WPWP planktonic stack constrained by radiocarbon data (1.50 to 3743 ka BP) to the equivalent portion of the benthic LR04 and LS16 global benthic $\delta^{18}O$ stacks (Lisiecki and Raymo, 2005; Lisiecki and Stern, 2016). The LS16 global stack is constructed with direct ^{14}C age constraints and is weighted towards the Pacific based on ocean basin volume, whereas the LR04 stack is based only on indirect age constraints and more heavily weighted toward Atlantic values (Lisiecki and Raymo, 2005; Lisiecki and Stern, 2016). However, all three age modelsstacks show good agreement for the timing of $\delta^{18}O$ change during Termination I, suggesting that age estimates for WPWP planktonic and benthic $\delta^{18}O$ are similar on orbital time scales (**Fig. 6**). PWe also compare changes in planktonic and benthic $\delta^{18}O$ were compared by depth inmeasured within individual WPWP stack cores as a function of depth for MD05-2925, ODP-1143, and ODP-806 (Lo et al., 2019; Lo, 2021; Tian et al., 2006; Lea et al., 2000; Medina-Elizalde and Lea, 2005; Bickert et al., 1993). These cores do not show a consistent lead/lag between the planktonic $\delta^{18}O$ and benthic $\delta^{18}O$ records (**Fig. S1 - S3**), further supportingadditionally indicating that on orbital time scales, the timing of WPWP planktonic and benthic $\delta^{18}O$ change is similar in the WPWPon orbital time scales.

The relative timing of millennial-scale variability between the WPWP planktonic stack and benthic $\delta^{18}O$ is more difficult to evaluate. Apparent differences in timing of a millennial-scale feature in the stacks between 36 and 38 ka may be an artifact of age model uncertainty. Age uncertainty for the LR04 stack beyond 30 ka is ± 4 kyr, and age estimates for the LS16 stack have a 95% confidence interval width of 2 to 4 kyr between 30 and 40 ka. Age estimates for that portion of our WPWP stack are not well constrained due to the scarcity of radiocarbon samples data available beyond 30 ka. The portions of our WPWP stack older than 3745 ka, which are not constrained by radiocarbon data, inherit the +/- 4 kyr age uncertainty of the LR04 stack used as the initial alignment target. Thus, we have no independent age estimates for WPWP planktonic $\delta^{18}O$ changes older than 3745 ka BP.

Formatted: Font color: Text 1
Formatted: Font: 10 pt
Formatted: Font: 10 pt
Formatted: Font: 10 pt
Formatted: Font: 10 pt, Font color: Text 1
Formatted: Font color: Text 1
Formatted: Font: 10 pt
Formatted: Font: 10 pt, Font color: Text 1
Formatted: Font color: Text 1
Formatted: Font: 10 pt, Font color: Text 1
Formatted: Font color: Text 1
Formatted: Font color: Text 1
Formatted: Font: 10 pt, Font color: Text 1
Formatted: Font color: Text 1
Formatted: Font color: Text 1
Formatted: Font: 10 pt
Formatted: Font color: Text 1
Formatted: Font: 10 pt
Formatted: Font color: Text 1
Formatted: Font: 10 pt, Font color: Text 1
Formatted: Font color: Text 1
Formatted: Font: 10 pt, Font color: Text 1
Formatted: Font color: Text 1
Formatted: Font: 10 pt
Formatted: Font color: Text 1
Formatted: Font: 10 pt, Font color: Text 1
Formatted: Font color: Text 1
Formatted: Font: 10 pt
Formatted: Font: 10 pt
Formatted: Font: 10 pt

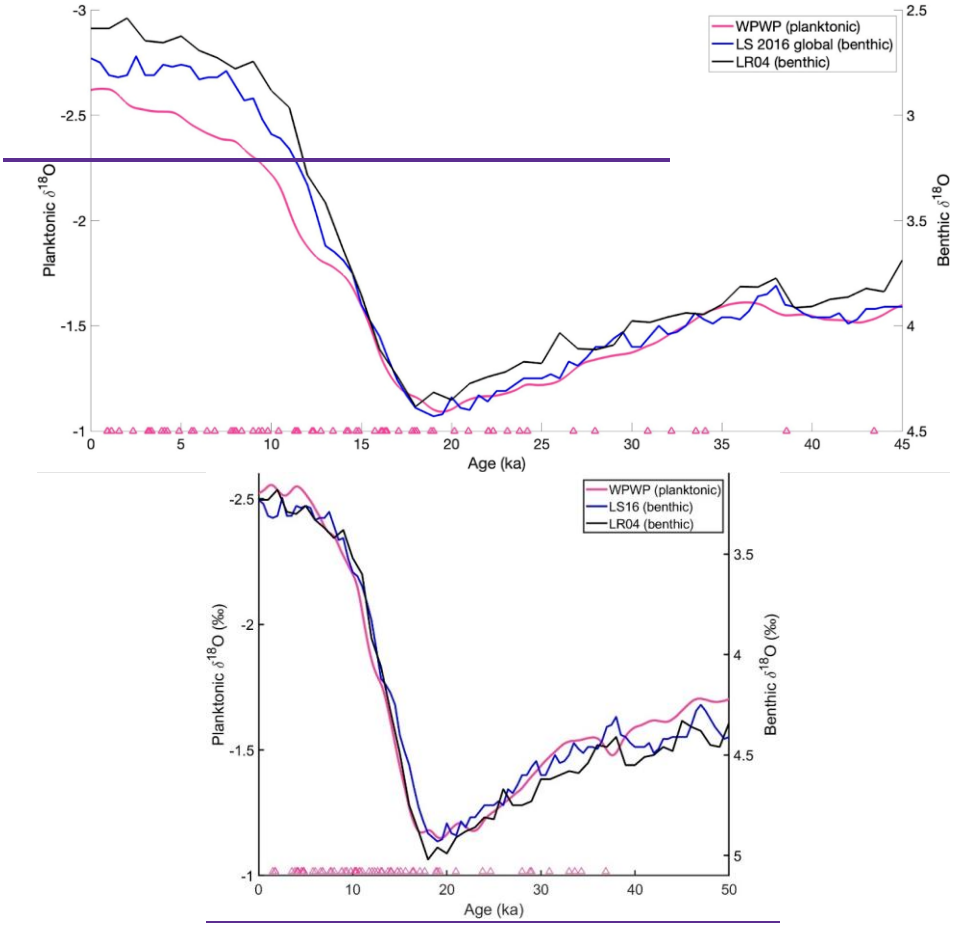

Figure 6. ~~Our~~ The **WPWP planktonic δ^{18}O stack (pink) compared to the global benthic δ^{18}O stacks** of Lisiecki and Stern (2016) (blue) and Lisiecki and Raymo (2005) (black) ~~with a shift of -0.5 ‰ and Lisiecki and Raymo (2005) (black) with a shift of -0.6 ‰~~. Triangles represent radiocarbon ages included in our WPWP stack construction (Oppo et al., 2003; ~~Holbourn et al., 2005; Jian et al., 2022;~~ Lo et al., 2017; Regoli et al., 2015; Dang et al., 2020; Zhang et al., 2021).

Formatted: Centered

Formatted: Font: Bold

Formatted: Not Highlight

Formatted: Not Highlight

6.2 Application of BIGMACS to pPlanktonic $\delta^{18}O$

6.2.1 Standard dDeviation of pPlanktonic vVersus bBenthic sStacks

The new Bayesian alignment software BIGMACS has previously only been applied to benthic $\delta^{18}O$ data (Lee and Rand et al., 20223accepted), and this study is the first to use the software to stack planktonic $\delta^{18}O$ data. To evaluate the performance of BIGMACS in stacking WPWP benthic and planktonic $\delta^{18}O$, we compare the average standard deviation of the new WPWP planktonic $\delta^{18}O$ stack to two benthic $\delta^{18}O$ stacks constructed with BIGMACS using six cores from the Deep Northeast Atlantic (DNEA stack) and four cores from the Intermediate Tropical Western Atlantic (ITWA stack). Based on the BIGMACS assumption of homogeneity across aligned records, all $\delta^{18}O$ residuals are assumed to be internal errors associated with sampling noise and measurement uncertainty and, thus, all residuals contribute similarly to estimating the stack's time-dependent standard deviation. A similar standard deviation for $\delta^{18}O$ in the stacks would indicate a similar signal-to-noise ratio in the stacked data, suggesting a similar effectiveness in the stacking process.

The DNEA and ITWA stacks have mean standard deviations of 0.13 ‰ and 0.2 ‰, respectively, for 0 to 60 ka (Lee and Rand et al., 20223accepted), while the newour WPWP planktonic stack has a mean standard deviation of 0.16 5‰ for the same age range. A larger mean standard deviation of 0.19 20‰ for the full age range of 0 to 800 ka for our WPWP stack is likely due in part to the lower resolution of data used in the second half of the stack; however, it is still similar to the standard deviation of the ITWA benthic stack. The similar $\delta^{18}O$ standard deviations for the planktonic and benthic stacks suggests that BIGMACS may be similarly effective at aligning and stacking homogeneous regional planktonic $\delta^{18}O$ data as regional benthic $\delta^{18}O$ data. However, before stacking either benthic or planktonic $\delta^{18}O$ records, BIGMACS users should carefully evaluate whether the records to be aligned and stacked are homogeneous (i.e., share a common and synchronous signal).

6.2.2 Homogeneity of WPWP pPlanktonic $\delta^{18}O$

The process of stack construction assumes that all included WPWP planktonic $\delta^{18}O$ records used have one homogeneous signal, i.e., that they all share the same underlying signal (with allowance for site-specific shift and scale values caused by), but physical processes, such as temperature and salinity gradients, could create variation between the WPWP core locations). The shift and scale values calculated for each record during stack construction can be used as an estimate of how similar or different the means and amplitudes of the planktonic $\delta^{18}O$ signals are between cores. The shift values of the 101 cores in the WPWP stack range between -0.62 and 0.6456 ‰, and scale values adjust the amplitudes of the signals by a factor of range from 0.72 to 1.1109 (**Table 2**). The benthic DNEA and ITWA stacks constructed using BIGMACS have a smaller range of shift and scale parameters than the WPWP stack. S, with shift values rangeing from -0.07 to 0.25 ‰ and -0.25 to 0.3 ‰ for the DNEA and ITWA stacks, respectively (Lee and Rand et al., 20223accepted); b. Benthic scale values vary range between 0.92 to 1.04 for the DNEA stack and 0.91 to 1 for the IWTWA stack (Lee and Rand et al., 20223accepted). Thus, the core-specific shift and scale values suggest more spatial variability in WPWP planktonic $\delta^{18}O$ than in regional benthic $\delta^{18}O$ compilations.

WPWP cores ODP 124 769A and MD97-2141, both of which are located in the Sulu Sea, have two of the largestmost negative shifts and smallest scale values (Linsley et al., 1991; Oppo et al., 2003). Cores KX21-2, KX22-4 and ODP-806, located in the eastern, open ocean portion of the WPWP, also have small scale values and negative shifts (Dang et al., 2020; Zhang et al., 2021; Lea et al., 2000; Medina-ElizaldeLea and Leaet al., 20050). The similar shift and scale values for pairs of neighboringneighboring cores with different data resolution suggest that these results reflect real differences in SST or salinity variability within the WPWP and indicate a weaker amplitude for planktonic $\delta^{18}O$ change at these sites. Previous studies show regional differences in $\delta^{18}O_{seawater}$ that may explain the reduced amplitude of planktonic $\delta^{18}O$ change at sites in the Sulu Sea and eastern WPWP (Lea et al., 2000; de Garidel-Thoron et al., 2005). Unlike the central and southern WPWP where glacial surface water $\delta^{18}O$ shiftedwas more toward more positive valueslly at the LGM (Visser et al., 2003; Xu et al., 2008, Li et al. 2016), these sites, ODP-769A, MD97-2141, KX21-2, KX22-4 and ODP-806, show negative shifts in surface water $\delta^{18}O$ at the LGM (Rosenthal et al., 2003; Lea et al., 2000). The observed heterogeneity in $\delta^{18}O_{seawater}$ likely results

Formatted: Font color: Text 1
Formatted: Font color: Text 1
Formatted: Font color: Text 1
Formatted: Font color: Text 1
Formatted: Font: 10 pt
Formatted: Font: 10 pt
Formatted: Font: 10 pt, Not Highlight
Formatted: Font: 10 pt
Formatted: Font: 10 pt
Formatted: Font color: Text 1
Formatted: Font color: Text 1
Formatted: Font: (Default) +Body (Times New Roman), 10 pt
Formatted: Font: 10 pt
Formatted: Font: (Default) +Body (Times New Roman), 10 pt
Formatted: Font: (Default) +Body (Times New Roman), 10 pt
Formatted: Font: (Default) +Body (Times New Roman), 10 pt, Font color: Text 1
Formatted: Font: 10 pt, Font color: Text 1
Formatted: Font: 10 pt
Formatted: Font: (Default) +Body (Times New Roman), 10 pt
Formatted: Font: 10 pt
Formatted: Font: 10 pt, Not Highlight
Formatted: Font: 10 pt
Formatted: Font: 10 pt, Bold
Formatted: Font: 10 pt
Formatted: Font: 10 pt
Formatted: Font: 10 pt
Formatted: Font: 10 pt, Not Bold
Formatted: Font: 10 pt
Formatted: Font: 10 pt
Formatted: Font: 10 pt
Formatted: Font: 10 pt
Formatted: Font: 10 pt, Font color: Text 1
Formatted: Font color: Text 1
Formatted: Font: 10 pt, Font color: Text 1
Formatted: Font: 10 pt

from regional differences in precipitation (de Garidel-Thoron et al., 2005) and/or the varied impacts of changes in sea level on the Indonesian throughflow and connectivity of regional seas (Linsley et al., 2010).

Although alignment of $\delta^{18}O$ signals for stacking requires an assumption that the WPWP planktonic $\delta^{18}O$ is homogenous, the BIGMACS estimated core-specific shift and scale parameters should still allow us to ~~still~~ extract the underlying signal common to the region despite small differences in the mean and amplitude of the signal among core sites. The similar standard deviation for the planktonic stack compared to benthic stacks suggests that the shift and scale factors are effective for identifying a common, shared planktonic $\delta^{18}O$ signal across the WPWP.

More variability in the planktonic $\delta^{18}O$ data is expected because the surface ocean composition has greater spatial variability due to factors like temperature and salinity than the deep ocean, which could account for some of the disparity in shift and scale values of the benthic versus planktonic data. The greater spatial variability in planktonic data is one reason why regional planktonic stacks ~~would be~~are more useful than global planktonic stacks. By describing regional patterns of response, regional planktonic stacks can improve age models based on stratigraphic alignment. The higher resolution, 0 to~~-~~ 450 ka portion of our WPWP stack may be particularly useful for this purpose. Although the new WPWP planktonic stack can improve estimates of relative age regionally, we caution that its absolute ages are susceptible to our assumption of synchronous change in benthic $\delta^{18}O$ and WPWP planktonic $\delta^{18}O$ and the absolute age uncertainty of the LR04 stack.

6.2.3 Planktonic vs. ~~b~~Benthic ~~a~~Alignment ~~u~~Uncertainty

Here we compare the ~~alignment~~age uncertainty during planktonic versus benthic ~~stack construction~~alignment in BIGMACS. ~~evaluate whether the spatial variability of WPWP planktonic $\delta^{18}O$ and its amplitude lead to systematic differences in the uncertainty of core alignments for planktonic versus benthic stack construction.~~ The average 95% confidence interval width for alignment uncertainty across all WPWP cores is 4.8 kyr for the full length of the WPWP stack and 4.4 kyr for the 0 to ~~-~~ 450 kyr portion of the stack, which has higher resolution data. Similarly, a North Atlantic benthic $\delta^{18}O$ stack also constructed using BIGMACS has an average alignment uncertainty of 4.4 kyr for the 0 to~~-~~ 654 ka length of that stack (Hobart et al., 2023). Thus, despite differences in the amplitude and spatial variability of WPWP planktonic $\delta^{18}O$ compared to North Atlantic benthic $\delta^{18}O$, ~~we find that BIGMACS~~ alignment uncertainty is similar for the construction of planktonic and benthic~~for WPWP planktonic $\delta^{18}O$ is similar to the uncertainty associated with benthic~~ $\delta^{18}O$ stack~~s construction~~. During most of the stack construction process, all records used for alignment are exclusively planktonic or benthic $\delta^{18}O$. (Although the LR04 benthic stack is used as the initial alignment target for the WPWP stack, the BIGMACS alignment target is updated to reflect the mean planktonic $\delta^{18}O$ signal during each iteration of stack construction.~~)~~

BIGMACS assumes that the records used for alignment share the same underlying signals; therefore, alignment should be more reliable with smaller uncertainties when a nearb~~(~~y planktonic $\delta^{18}O$ record is aligned to the WPWP planktonic stack rather than the LR04 benthic stack. We demonstrate the potential impacts of aligning to different stacks by comparing the age estimates for the planktonic $\delta^{18}O$ record of core MD01-2378 (Holbourn et al., 2005) from the Timor Sea (slightly outside the boundaries of the WPWP) based on alignment to either the WPWP stack or the LR04 stack (Bowman et al., 2023). Differences between the features of the two stacks during MIS 3 and 4 produce a ~14 kyr error in the alignment of the core to the LR04 stack ~~at ~77 kyr ago~~, as indicated by the shifted position of the dashed vertical line in (~~Fig. 7~~). The proper alignment of MIS 4 to the WPWP stack produces a 95-% CI width of 6.5 kyr for estimated age at that time, compared to a 95 % CI width~~s~~ of 13 to 18 kyr associated with the incorrect alignment to the LR04 stack. Because the planktonic $\delta^{18}O$ records near the WPWP share features which differ from those of benthic $\delta^{18}O$, age model results for WPWP cores ~~are expected~~should be more accurate when the~~ir~~se planktonic $\delta^{18}O$ records are aligned to the WPWP stack than to a benthic stack.

Formatted: Font color: Text 1
Formatted: Font color: Text 1
Formatted: Font: 10 pt
Formatted: Font: 10 pt
Formatted: Font: 10 pt
Formatted: Font: 10 pt

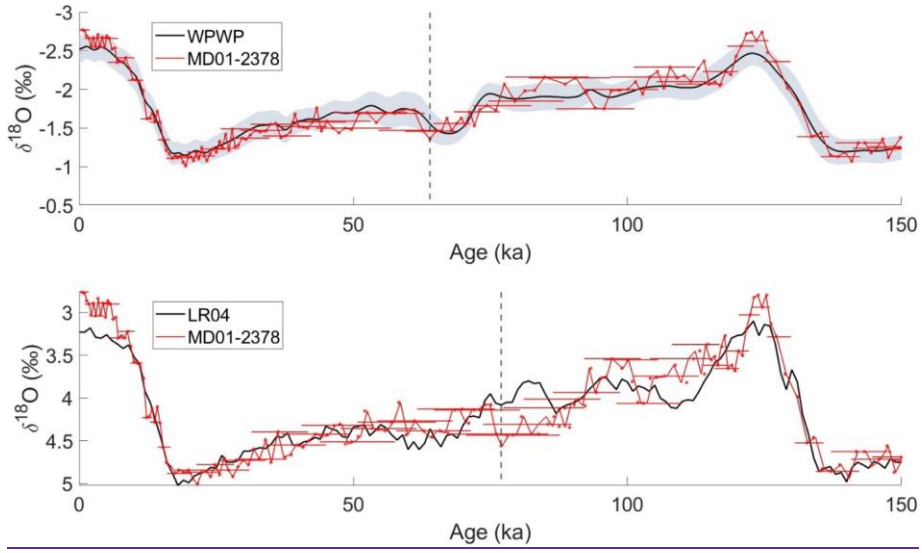

Figure 7. MD01-2378 alignment target comparison. (top) Planktonic δ^{18}O for Timor Sea (near WPWP) core MD01-2378 (red, Holbourn et al., 2005) aligned to the WPWP planktonic δ^{18}O WPWP stack (black, with gray shading for 1-standard deviation in δ^{18}O) (Holbourn et al., 2005). Asterisks indicate MD01-2378 planktonic δ^{18}O samples. Horizontal error bars representing the MD01-2378 δ^{18}O alignment uncertainty at every 3rd δ^{18}O point (uncertainty shown at ½ resolution to improve figure legibility). Regional planktonic δ^{18}O WPWP stack (black) with 1 standard deviation δ^{18}O alignment uncertainty shading. (bottom) Planktonic δ^{18}O for Timor Sea (near WPWP) core MD01-2378 (red, Holbourn et al., 2005) aligned to the benthic δ^{18}O LR04 stack . Asterisks indicate MD01-2378 planktonic δ^{18}O samples. Horizontal error bars representing the MD01-2378 δ^{18}O alignment uncertainty at every 3rd δ^{18}O point (uncertainty shown at ½ resolution to improve figure legibility). Global benthic δ^{18}O LR04 stack (black, Lisiecki and Raymo, 2005). In both panels, r(both) ed symbols mark MD01-2378 planktonic δ^{18}O samples with shift and scale applied to match the respective alignment targets. Horizontal error bars indicate the 95% CI alignment uncertainty for every third δ^{18}O measurement (to improve figure legibility). VThe vertical dashed lines indicate a planktonic δ^{18}O feature inmark two different alignments of 8.81 m depth in MD01-2378, at 8.81 m depth with an age ofwhich shifts from 64 ka when aligned to the WPWP planktonic stack compared to an age ofto 77 ka when aligned to the LR04 benthic stack.

6.3 Contributions of SST and iIce vVolume to WPWP pPlanktonic δ^{18}O

A recent study by Jian et al. (2022) constructed an IPWPWP SST stack from 0 to -360 ka. We compare the orbital-scale variability between the SST stack and our planktonic δ^{18}O stack using spectral analysis and by converting the SST stack change to $\Delta\delta^{18}O_{SST}$, which is an estimate of the oxygen isotope fractionation in foraminiferal carbonate caused by SST. Many of the same features can be seen in the WPWP stacks of planktonic δ^{18}O and SST (**Fig. 987, top**upper panel); however, the planktonic δ^{18}O values of the last two interglacials are similar to one another whereas Holocene SST for the Holocene is notably cooler than the SST for of the penultimate interglacial. The WPWP planktonic δ^{18}O and SST stacks have similar proportions of normalized spectral power at orbital frequencies, but SST has slightlyslightly less 41kyr obliquity power and slightly more precession power **(Fig. 98).**

Formatted: Centered

Formatted: Font: 9 pt
Formatted: Font color: Text 1
Formatted: Font: 9 pt
Formatted: Font color: Text 1
Formatted: Font: 9 pt
Formatted: Font color: Text 1
Formatted: Font: 9 pt
Formatted: Font color: Text 1
Formatted: Font: 9 pt
Formatted: Font color: Text 1
Formatted: Font color: Text 1
Formatted: Font color: Text 1
Formatted: Font color: Text 1
Formatted: Font color: Text 1
Formatted: Font color: Text 1
Formatted: Font: 9 pt
Formatted: Font color: Text 1
Formatted: Font color: Text 1
Formatted: Font: 10 pt
Formatted: Font: 10 pt
Formatted: Font: 10 pt

To estimate the combined effects of SST and ice volume change, the ~~I~~WPWP $\Delta\delta^{18}O_{SST}$ was added to an estimate of $\Delta\delta^{18}O_{ice}$ (**Fig. ~~8~~7, bottom**) from a global sea level (ice volume) stack (Spratt and Lisiecki, 2016). The combined SST and ice volume $\Delta\delta^{18}O_{SST+ice}$ should represent the majority of the planktonic $\delta^{18}O$ change in our WPWP planktonic $\delta^{18}O$ stack, except for salinity-induced changes. The two combined $\Delta\delta^{18}O$ components show similar glacial/interglacial cyclicity and timing of change as our WPWP planktonic $\delta^{18}O$ stack but with a slightly larger amplitude, particularly during MIS 2 and 3 (20 to 70 ka), MIS 7 (200 to 250 ka) and MIS 9 (310 to 330 ka). Salinity-induced changes in the $\delta^{18}O$ of WPWP surface water may offset some of the WPWP $\Delta\delta^{18}O_{SST+ice}$ signal. However, some of the discrepancy could also be explained by spatial variability in the ~~WPWP~~ IPWP if the sites used for our WPWP planktonic $\delta^{18}O$ stack had less average SST change than those in the IPWP SST stack (Jian et al., 2022).

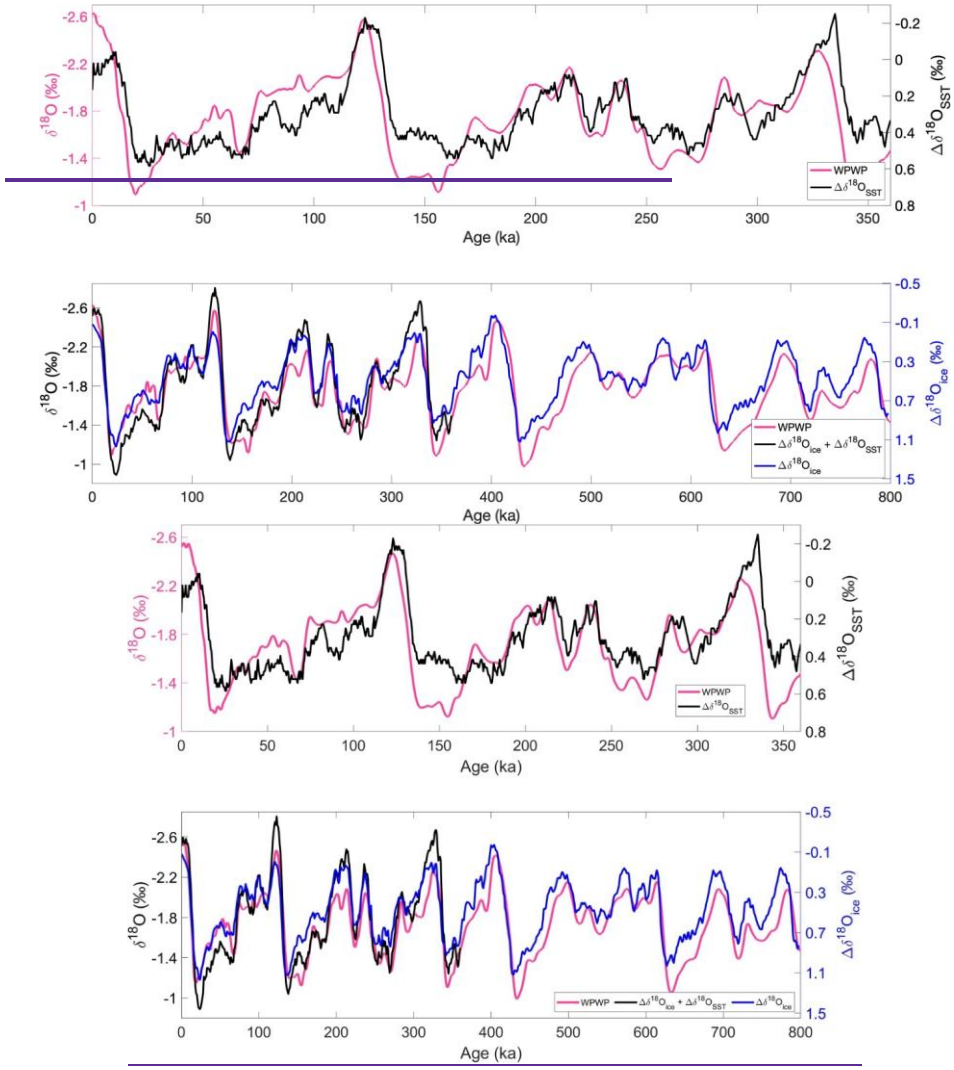

Figure 87. Ice volume and temperature c~~C~~ontributions to WPWP planktonic $\delta^{18}O_c$ (top) The WPWP planktonic $\delta^{18}O$ stack (pink) and the ~~I~~WPWP SST stack of Jian et al. 2022, on its original age model and converted to $\Delta\ \delta^{18}O$ per mil-equivalent (black). (bottom) The

Formatted: Centered

Formatted: Font: Bold

WPWP stack (pink) compared to a sea level stack (Spratt and Lisiecki, 2016) converted to $\Delta\delta^{18}O_{ice}$ per mil-equivalent (blue), and the sum of $\Delta\delta^{18}O_{SST}$ and $\Delta\delta^{18}O_{ice}$ change (black).

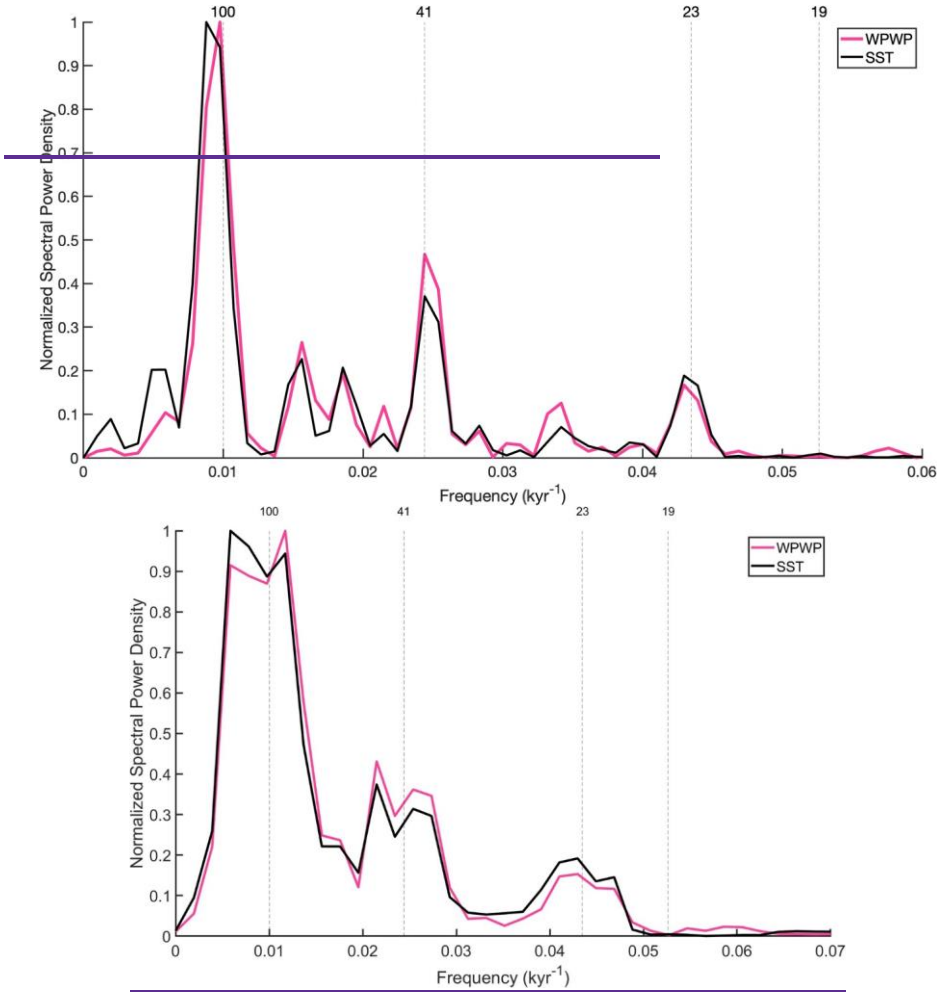

Figure 98. Normalized power spectral density of the WPWP planktonic $\delta^{18}O$ stack (pink) and IWPWP SST stack (black, Jian et al., 2022) from 0 to -360 ka for both stacks using MATLAB's ptmtm( ) function (MATLABThe Mathworks Inc., R2023a2b). Orbital frequencies that correspond to 100, 41, 23 and 19 kyr are marked by vertical dashed lines.

Formatted: Centered

7 Data aAvailability

The WPWP planktonic $\delta^{18}O$ stack ~~can~~ be accessed on Zenodo with the DOI https://doi.org/10.5281/zenodo.10211900 ~~https://doi.org/10.5281/zenodo.8190829~~ (Bowman et al., 2023) in the "WPWP_planktonic_stack.txt" file, which contains the age, mean $\delta^{18}O$, and the $\delta^{18}O$ standard deviation. The same file is also available as "stack.txt" in ~~the 'Output' folder~~the WPWP_10cores_v12_stack_output.zip file. The previously published depth and planktonic $\delta^{18}O$ data as well as any radiocarbon or tie points for each core used during stack construction can be found as .txt files in the 'Inputs' folder. ~~BIGMACS~~ BIGMACS-produced age models, depth, calibrated radiocarbon ages, and planktonic $\delta^{18}O$ data for each core can be found in the 'Outputs' folder in the "results.mat" file and as .txt files in the individual folders named for each core.

The planktonic $\delta^{18}O$ alignments for core MD01-2378 (Holbourn et al., 2005) to both the WPWP planktonic $\delta^{18}O$ stack and the LR04 benthic $\delta^{18}O$ stack (Lisiecki and Raymo, 2005) can also be accessed at the ~~following~~ DOI: ~~https://doi.org/10.5281/zenodo.10211900~~https://doi.org/10.5281/zenodo.10211900. The BIGMACS-produced age model~~,~~ and the ~~depth, and the planktonic $\delta^{18}O$ and radiocarbon~~ data used ~~during~~for the alignment can be found in the "results.mat" file of the "MD01-2378_WPWPalignment_output.zip" (or "…LR04alignment_output") files. The ~~same~~ age model ~~and depth data~~results can also be found in text file form in the "Ages" folder of the output folders. The ~~same~~ depth, radiocarbon, and planktonic $\delta^{18}O$ data used for alignments can ~~also~~ be ~~can be~~ found in text file form in the "MD01-2378" folder of the "MD01-2378_WPWPalignment_input.zip" (or "…LR04alignment_input") files.

The alignment software BIGMACS (Lee and Rand et al., 2023) used to construct our WPWP stack can be downloaded at ~~the following DOI:~~ https://github.com/eilion/BIGMACS. ~~(Lee and Rand et al., 2023accepted).~~

8 Conclusions

We present a regional planktonic $\delta^{18}O$ stack of the ~~West Pacific~~Western Pacific Warm Pool constructed from ~~eleven~~ ten previously published cores using the new alignment software BIGMACS (Lee and Rand et al., ~~accepted~~20232). The stack age model is constrained by 6~~5~~7 radiocarbon dates from 1.5~~0.89~~ to~~-~~ 37~~43.46~~ ka ~~BP~~ in four WPWP cores and otherwise follows the age model of the LR04 benthic $\delta^{18}O$ stack (Lisiecki and Raymo, 2005). Within the radiocarbon time interval, the timing of WPWP planktonic $\delta^{18}O$ appears nearly synchronous with global mean benthic $\delta^{18}O$ change. The WPWP planktonic $\delta^{18}O$ stack provides a useful regional alignment target for WPWP planktonic $\delta^{18}O$ records, particularly for the 0 to~~-~~ 450 ka portion which has a~~is~~ higher resolution than the older portion of the stack. Future improvements to the WPWP stack could include higher resolution planktonic $\delta^{18}O$ in the older portion of the stack and better~~more~~ age constraints beyond 37~~25~~ ka ~~BP~~.

Analyses of the stack's standard deviation and alignment uncertainty suggest that BIGMACS performs similarly well stacking WPWP planktonic $\delta^{18}O$ as it does for regional benthic $\delta^{18}O$ data. The new stack ~~demonstrates~~ has weaker glacial~~/-~~interglacial amplitudes and orbital power for WPWP planktonic $\delta^{18}O$ change than benthic $\delta^{18}O$ stacks over the last 800 ka~~yr~~. WPWP planktonic $\delta^{18}O$ change is also somewhat weaker than estimated based on global ice volume and ~~I~~WPWP SST change, perhaps due to spatial heterogeneity or surface salinity change. Differences in glacial-interglacial amplitudes between the WPWP planktonic stack and benthic $\delta^{18}O$ stacks validate that these differences are characteristic of planktonic $\delta^{18}O$ throughout the WPWP. Furthermore, stratigraphic alignments of planktonic $\delta^{18}O$ from cores near the WPWP ~~will~~should ~~be~~produce more reliable relative age estimates when aligned to the WPWP planktonic stack instead of a benthic $\delta^{18}O$ stack.

Author c~~C~~ontribution

CLB curated the previously published data, performed the formal analysis, visualization, and prepared the original draft. DSR was involved with age model methodology/software development, visualization, and manuscript review and editing. LEL conceptualized the project, supervised, and contributed to the original draft preparation and manuscript review and editing. SCB provided validation and manuscript review and editing.

Formatted: Font color: Text 1
Formatted: Font: 10 pt
Formatted: Font: 10 pt
Formatted: Font: 10 pt
Formatted: Font: 10 pt
Formatted: Default Paragraph Font, Font: 12 pt, Font color: Auto
Formatted: Font: 10 pt
Formatted: Indent: First line: 0"
Formatted: Font: 10 pt
Formatted: Font: 10 pt, Font color: Text 1
Formatted: Font color: Text 1
Formatted: Font: 10 pt
Formatted: Font: 10 pt
Formatted: Font: 10 pt
Formatted: Font: 10 pt
Formatted: Font: 10 pt
Formatted: Font: 10 pt

Competing i~~I~~nterests
The authors declare that they have no conflict of interest.

Acknowledgments
This work was supported in part by the National Science Foundation (NSF) under the project number OCE-1760878.

References

Bemis, B. E., Spero, H. J., Bijma, J., and Lea, D. W.: Reevaluation of the oxygen isotopic composition of planktonic foraminifera: Experimental results and revised paleotemperature equations, Paleoceanogr., 13, 150-160, https://doi.org/10.1029/98PA00070, 1998.

Bickert, T., Berger, W. H., Burke, S., Schmidt, H., and Wefer, G.: (Appendix A) Stable oxygen and carbon isotope ratios of Cibicidoides wuellerstorfi from ODP Hole 130-806B on the Ontong Java Plateau. PANGAEA [data set], https://doi.org/10.1594/PANGAEA.696408, 1993.

Bowman, C. L., Rand, D. S., Lisiecki, L. E., and Bova, S. C.: An 800 kyr planktonic $\delta^{18}O$ stack for the West Pacific Warm Pool, Zeodo [data set], https://doi.org/10.5281/zenodo.10211900, 2023.

Broccoli, A. J.: Tropical Cooling at the Last Glacial Maximum: An atmosphere–mixed layer ocean model simulation, J. Clim., 13, ~~951–976,~~ 951–976, ~~https://doi.org/10.1175/1520-0442(2000)013~~ https://doi.org/10.1175/1520-0442(2000)013<0951:TCATLG>2.0.CO;2, 2000.

Channell, J. E. T., Hodell, D. A., Singer, B. S., and Xuan, C.: Reconciling astrochronological and 40Ar/39Ar ages for the Matuyama-Brunhes boundary and Late Matuyama Chron, Geochem., Geophys., Geosyst., 11, Q0AA12, https://doi.org/10.1029/2010GC003203, 2010.

Chuang, C., Lo, L., Zeeden, C., Chou, Y., Wei, K., Shen, C., Mii, H., Chang, Y., and Tung, Y.: Integrated stratigraphy of ODP Site 1115 (Solomon Sea, southwestern equatorial Pacific) over the past 3.2 Ma., Mar. Micropaleonto., 144, 25-37, https://doi.org/10.1016/j.marmicro.2018.09.003, 2018.

Chuang, C., Lo, L., Zeeden, C., Chou, Y., Wei, K., Shen, C., Mii, H., Chang, Y., and Tung, Y.: Isotopic analysis of Globigerinoides sacculifer from ODP Hole 180-1115B, PANGAEA [data set], https://doi.org/10.1594/PANGAEA.899187, 2019.

Conroy, J. L., Cobb, K. M., Lynch-Stieglitz, J., and Polissar, P. J.: Constraints on the salinity–oxygen isotope relationship in the central tropical Pacific Ocean, Mar. Chem., 161, 26–33, https://doi.org/10.1016/j.marchem.2014.02.001, 2014.

Dang, H., Wu, J., Xiong, Z., Qiao, P., Li, T., and Jian, Z.: Orbital and sea-level changes regulate the iron-associated sediment supplies from Papua New Guinea to the equatorial Pacific, Quat. Sci. Rev., 239, 106361, https://doi.org/10.1016/j.quascirev.2020.106361, 2020.

Dang, H., Wu, J., Xiong, Z., Qiao, P., Li, T., and Jian, Z.: Oxygen isotopes of Globigerinoides ruber from core KX21-2 from the western equatorial Pacific over the last ~400 ka, PANGAEA [data set], https://doi.org/10.1594/PANGAEA.922658, 2020.

De Deckker, P.: The Indo-Pacific Warm Pool: critical to world oceanography and world climate, Geosci. Lett., 3, 20, https://doi.org/10.1186/s40562-016-0054-3, 2016.

de Garidel-Thoron, T., Rosenthal, Y., Bassinot, F., and Beaufort, L.: Stable sea surface temperatures in the Western Pacific Warm Pool over the past 1.75 million years, Nat., 433, 294–298, https://doi.org/10.1038/nature03189, 2005.

de Garidel-Thoron, T., Rosenthal, Y., Bassinot, F.C., and Beaufort, L.: Western Pacific Warm Pool Pleistocene paired $\delta^{18}O$ -Mg/Ca and SST reconstruction, NOAA National Centers for Environmental Information [data set], https://doi.org/10.25921/ejer-t729, 2005.

de Garidel-Thoron, T., Rosenthal, Y., Beaufort, L., Bard, E., Sonzogni, C., and Mix, A. C.: A multiproxy assessment of the western equatorial Pacific hydrography during the last 30 Kyr, Paleoceanogr., 22, PA3204, https://doi.org/10.1029/2006PA001269, 2007.

Heaton, T. J., Köhler, P., Butzin, M., Bard, E., Reimer, R. W., Austin, W. E. N., Ramsey, C. B., Grootes, P. M., Hughen, K. A., Kromer, B., Reimer, P. J., Adkins, J., Burke, A., Cook, M. S., Olsen, J., and Skinner, L. C.: Marine20—The marine radiocarbon age calibration curve (0–55,000 Cal BP), Radiocarbon, 62, 779–820, https://doi.org/10.1017/RDC.2020.68, 2020.

Hobart, B., Lisiecki, L.E., Rand, D., Lee, T., and Lawrence, C. E.: Late Pleistocene 100-kyr glacial cycles paced by precession forcing of summer insolation, Nat. Geosci., 16, 717–722, https://doi.org/10.1038/s41561-023-01235-x, 2023.

Holbourn, A., Kuhnt, W., Kawamura, H., Jian, Z., Grootes, P., Erlenkeuser, H., and Xu, J.: Orbitally paced paleoproductivity variations in the Timor Sea and Indonesian Throughflow variability during the last 460 Kyr, Paleoceanogr., 20, PA3002, https://doi.org/10.1029/2004PA001094, 2005.

Holbourn, A. E., Kuhnt, W., Kawamura, H., Jian, Z., Grootes, P. M., Erlenkeuser, H., and Xu, J.: Stable isotopes on planktic foraminifera of sediment core MD01-2378, PANGAEA [data set], https://doi.org/10.1594/PANGAEA.263757, 2005.

Hollstein, M., Mohtadi, M., Kienast, M., Rosenthal, Y., Groeneveld, J., Oppo, D. W., Southon, J. R., and Lückge, A.: The impact of astronomical forcing on surface and thermocline variability within the Western Pacific Warm Pool over the past 160 Kyr, Paleoceanogr. and Paleoclimatol., 35, e2019PA003832, https://doi.org/10.1029/2019PA003832, 2020.

Huybers, P., and Wunsch, C.: A depth-derived Pleistocene age model: Uncertainty estimates, sedimentation variability, and nonlinear climate change, Paleoceanogr., 19, PA1028, https://doi.org/10.1029/2002PA000857, 2004.

Kuhnt, W., Holbourn, A., Xu, J., Opdyke, B., De Deckker, P., Rohl, U., and Mudelsee, M.: Southern Hemisphere control on Australian monsoon variability during the late deglaciation and Holocene, Nat. Commun., 6, 5916, https://doi.org/10.1038/ncomms6916, 2015.

Imbrie, J., Hays, J. D., Martinson, D. G., McIntyre A., Mix A. C., Morley, J. J., Pisias N. G., Prell, W. L., and Shackleton, N. J.: The orbital theory of Pleistocene climate: Support from a revised chronology of the marine $\delta^{18}O$ record, Milankovitch and Climate, Part 1, edited by: Berger, A., Imbrie, J., Kukla, G., Saltzman, B., and Reidel, D., Publishing Company, Dordrecht, Netherlands, 269-305, ISBN 9027717915, 1984.

Jian, Z., Wang, Y., Dang, H., Mohtadi, M., Rosenthal, Y., Lea, D. W., Liu, Z., Jin, H., Ye, L., Kuhnt, W., and Wang, X.: Warm Pool ocean heat content regulates ocean–continent moisture transport, Nat., 612, 92–99, https://doi.org/10.1038/s41586-022-05302-y, 2022.

Lee, T., Rand, D., Lisiecki, L. E., Gebbie, G., and Lawrence, C.: Bayesian age models and stacks: combining age inferences from radiocarbon and benthic $\delta^{18}O$ stratigraphic alignment, Clim. Past, 19, 1993–2012, https://doi.org/10.5194/cp-19-1993-2023, 2023.

Lea, D. W.: The 100,000-Yr Cycle in tropical SST, greenhouse forcing, and climate sensitivity, J. Clim., 17, 2170–2179, https://doi.org/10.1175/1520-0442(2004)017<2170:TYCITS>2.0.CO;2, 2004.

Lea, D. W., Pak, D. K., and Spero, H. J.: Climate impact of Late Quaternary equatorial Pacific sea surface temperature variations, Science, 289, 1719–1724, https://doi.org/10.1126/science.289.5485.1719, 2000.

Li L., Li, Q., Tian, J., Wang, P., Wang, H., and Liu, Z.: A 4-Ma record of thermal evolution in the tropical western Pacific and its implications on climate change, Earth and Planet. Sci. Lett., 309, 10-20, doi.org/10.1016/j.epsl.2011.04.016, 2011.

Li, Z.; Shi, X., Chen, M.-T.; Wang, H., Liu, S., Xu, J., Long, H., Troa, R. A., Zuraida, R., and Triarso, E.: Late Quaternary fingerprints of precession and sea level variation over the past 35 Kyr as revealed by sea surface temperature and upwelling records from the Indian Ocean near southernmost Sumatra, Quat. Int., 425, 282–291, https://doi.org/10.1016/j.quaint.2016.07.013, 2016.

Linsley, B. K., and M. T. von Breymann: Stable isotopic and geochemical record in the sulu sea during the last 750 k.y.:Assessment of surface water variability and paleoproductivity changes, Proceedings of the Ocean Drilling Program, Scientific Results, 24, 379-396, https://doi.org/10.2973/odp.proc.sr.124.151.1991, 1991.

Linsley, B., Rosenthal, Y., and Oppo, D.: Holocene evolution of the Indonesian Throughflow and the Western Pacific Warm Pool, Nat. Geosci., 3, 578–583, https://doi.org/10.1038/ngeo920, 2010.

Lisiecki, L. E., and Raymo, M. E.: A Pliocene-Pleistocene stack of 57 globally distributed benthic $\delta^{18}O$ records, Paleoceanogr., 20, PA1003, https://doi.org/10.1029/2004PA001071, 2005.

Lisiecki, L. E., and -Stern, J. V.: Regional and global benthic $\delta^{18}O$ stacks for the last glacial cycle, Paleoceanogr., 31, 1368–1394, https://doi.org/10.1002/2016PA003002, 2016.

Lo, L.: A dataset of the Mid-Brunhes period at site MD05-2925, Solomon Sea: Surface-subsurface planktonic foraminifera stable oxygen isotope and Mg/Ca ratios, Mendeley Data [data set], https://data.mendeley.com/datasets/9c2nnpchdh/1, 2021.

Lo, L., Chang, S., Wei, K., Lee, S., Ou, T., Chen, Y., Chuang, C., Mii, H., Burr, G. S., Chen, M., Tung, Y., Tsai, M., Hodell, D. A., and Shen, C.: Nonlinear climatic sensitivity to greenhouse gases over past 4 glacial/interglacial cycles, Sci. Rep., 7, 4626, https://doi.org/10.1038/s41598-017-04031-x, 2017.

Lo, L., Chang, S., Wei, K., Lee, S., Ou, T., Chen, Y., Chuang, C., Mii, H., Burr, G. S., Chen, M., Tung, Y., Tsai, M., Hodell, D. A., and Shen, C.: Age model and oxygen isotopes of planktonic foraminifera from sediment core MD05-2925 off the Solomon Sea, PANGAEA [data set], https://doi.org/10.1594/PANGAEA.899216, 2019.

Locarnini, R. A., Mishonov, A. V., Baranova, O. K., Boyer, T. P., Zweng, M. M., Garcia, H. E., Reagan, J. R., Seidov, D., K. Weathers, Paver, C. R., and Smolyar, I.: Temperature, world ocean atlas 2018, NOAA Atlas NESDIS 81 [data set], https://archimer.ifremer.fr/doc/00651/76338/, 2018.

Mayer, M., Haimberger L., and Balmaseda, M. A.: On the energy exchange between tropical ocean basins related to ENSO, J. Clim., 27, 6393–6403, https://doi.org/10.1175/JCLI-D-14-00123.1, 2014.

Medina-Elizalde, M., and Lea, D. W.: (Table S2) Stable oxygen isotope record and Mg/Ca ratios of Globigerinoides ruber from ODP Hole 130-806B. PANGAEA [data set], https://doi.org/10.1594/PANGAEA.772014, 2005.

Neale, R., and Slingo J.: The Maritime Continent and its role in the global climate: A GCM study, J. Clim., 16, 834–848, https://doi.org/10.1175/1520-0442(2003)016<0834:TMCAIR>2.0.CO;2, 2003.

Formatted ...
Formatted ...
Formatted ...
Formatted ...
Formatted ...
Formatted ...
Formatted ...
Formatted ...
Formatted ...
Formatted ...
Formatted ...
Formatted ...
Formatted ...
Formatted ...
Formatted ...
Formatted ...
Formatted ...
Formatted ...
Formatted ...
Formatted ...
Formatted: Font color: Text 1
Formatted: Font color: Text 1
Formatted: Font color: Text 1
Formatted: Font color: Text 1
Formatted: Font color: Text 1
Formatted: Font color: Text 1
Formatted: Font color: Text 1
Formatted: Font color: Text 1
Formatted: Font color: Text 1
Formatted: Font color: Text 1
Formatted: Font color: Text 1
Formatted: Font color: Text 1
Formatted: Font color: Text 1
Formatted: Font color: Text 1
Formatted: Font color: Text 1
Formatted: Font color: Text 1

Oppo, D. W., Linsley, B. K., Rosenthal, Y., Dannenmann, S., and Beaufort, L.: Orbital and suborbital climate variability in the Sulu Sea, western tropical Pacific, Geochem., Geophys., Geosyst., 4, 1–20, https://doi.org/10.1029/2001GC000260, 2003.

Oppo, D.W., Linsley, B.K., Rosenthal, Y., Dannenmann, S., and Beaufort, L.: Sulu Sea core MD97-2141 foraminiferal oxygen isotope data, NOAA National Centers for Environmental Information [data set], https://doi.org/10.25921/qqqx-kt90, 2003.

Past Interglacials Working Group of PAGES: Interglacials of the last 800,000 years, Rev. Geophys., 54, 162–219, https://doi.org/10.1002/2015RG000482, 2016.

Regoli, F., de Garidel-Thoron, T., Tachikawa, K., Jian, Z., Ye, L., Droxler, A. W., Lenoir, G., Crucifix, M., Barbarin, N., and Beaufort, L.: Progressive shoaling of the equatorial Pacific thermocline over the last eight glacial periods, Paleoceanogr., 30, 439–455, https://doi.org/10.1002/2014PA002696, 2015.

Rosenthal, Y., Oppo, D. W., and Linsley, B. K.: The amplitude and phasing of climate change during the last deglaciation in the Sulu Sea, western equatorial Pacific, Geophys. Res. Lett., 30, 1428, https://doi.org/10.1029/2002GL016612, 2003

Sadekov, A., Eggins, S. M., De Deckker, P., Ninnemann, U., Kuhnt, W., and Bassinot, F.: Surface and subsurface seawater temperature reconstruction using Mg/Ca microanalysis of planktonic foraminifera Globigerinoides ruber, Globigerinoides sacculifer, and Pulleniatina obliquiloculata, Paleoceanogr., 24, PA3201, https://doi.org/10.1029/2008PA001664, 2009.

Shakun, J. D., Lea, D. W., Lisiecki, L. E., and Raymo, M. E.: An 800-Kyr record of global surface ocean δ18O and implications for ice volume-temperature coupling, Earth and Planet. Sci. Lett., 426, 58–68, https://doi.org/10.1016/j.epsl.2015.05.042, 2015.

Singer, B. S.: A Quaternary geomagnetic instability time scale, Quat. Geochronol., 21, 29–52, https://doi.org/10.1016/j.quageo.2013.10.003, 2014.

Spero, H. J., Mielke, K. M., Kalve, E. M., Lea, D. W., and Pak, D. K.: Multispecies approach to reconstructing eastern equatorial Pacific thermocline hydrography during the past 360 Kyr, Paleoceanogr., 18, 1022, https://doi.org/10.1029/2002PA000814, 2003.

Spratt, R. M., and Lisiecki, L. E.: A Late Pleistocene sea level stack, Clim. Past, 12, 1079–1092, https://doi.org/10.5194/cp-12-1079-2016, 2016.

Tian, J. Pak, Dorothy K., Wang, P., Lea, D. W., Cheng, X., and Zhao, Q.: (Appendix 1) Stable oxygen isotope ratios of Globigerinoides ruber and benthic foraminifera from ODP Site 184-1143, PANGAEA [data set], https://doi.org/10.1594/PANGAEA.707833, 2006.

Tachikawa, K., Timmermann, A., Vidal, L., Sonzogni, C., and Timm, O. E.: CO2 radiative forcing and Intertropical Convergence Zone influences on Western Pacific Warm Pool climate over the past 400 ka, Quat. Sci. Rev., 86, 24–34, https://doi.org/10.1016/j.quascirev.2013.12.018, 2014.

The MathWorks Inc.: MATLAB version: 9.14.0 (R2023a), Natick, Massachusetts: The MathWorks Inc. https://www.mathworks.com, 2023.

Visser, K., Thunell, R., and Stott, L.: Magnitude and timing of temperature change in the Indo-Pacific Warm Pool during deglaciation, Nat., 421, 152–155, https://doi.org/10.1038/nature01297, 2003.

Wang, L.: Isotopic signals in two morphotypes of Globigerinoides ruber (white) from the South China Sea: Implications for monsoon climate change during the last glacial cycle, Paleoceanogr., Palaeoclimatol., Palaeoecol., 161, 381–394, https://doi.org/10.1016/S0031-0182(00)00094-8, 2000.

Formatted: Font color: Text 1

Wefer, G., and Berger, W. H.: Isotope paleontology: Growth and composition of extant calcareous species, Mar. Geol., 100, 207–248, https://doi.org/10.1016/0025-3227(91)90234-U, 1991

Xu, J., Holbourn, A., Kuhnt, W., Jian, Z., and Kawamura, H.: Changes in the thermocline structure of the Indonesian Outflow during terminations I and II, Earth and Planet. Sci. Lett., 273, 152–162, https://doi.org/10.1016/j.epsl.2008.06.029, 2008.

Zhang, S., Yu, Z., Gong, X., Wang, Y., Chang, F., and Li, T.: Sable oxygen isotope and Mg/Ca ratios of planktonic foraminifera from KX97322-4 (KX22-4), PANGAEA [data set], https://doi.org/10.1594/PANGAEA.939377, 2021.

Bemis, B. E., Spero, H. J., Bijma, J., Lea, D. W.: Reevaluation of the oxygen isotopic composition of planktonic foraminifera: Experimental results and revised paleotemperature equations, Paleoceanogr., 13(2), 150–160, https://doi.org/10.1029/98PA00070, 1998.

Bowman, C. L., Rand, D. S., Lisiecki, L. E., Bova, S. C.: An 800 kyr planktonic δ^{18}O stack for the West Pacific Warm Pool, Zeodo [data set], https://doi.org/10.5281/zenodo.8190829, 2023.

Channell, J. E. T., Hodell, D. A., Singer, B. S., Xuan, C.: Reconciling Astrochronological and 40Ar/39Ar Ages for the Matuyama-Brunhes Boundary and Late Matuyama Chron, Geochem., Geophys., Geosyst., 11 (12), https://doi.org/10.1029/2010GC003203, 2010.

Conroy, J. L., Cobb, K. M., Lynch-Stieglitz, J., Polissar, P. J.: Constraints on the Salinity–Oxygen Isotope Relationship in the Central Tropical Pacific Ocean, Mar. Chem., 161, 26–33, https://doi.org/10.1016/j.marchem.2014.02.001, 2014.

Dang, H., Wu, J., Xiong, Z., Qiao, P., Li, T., Jian, Z.: Orbital and Sea-Level Changes Regulate the Iron-Associated Sediment Supplies from Papua New Guinea to the Equatorial Pacific, Quat. Sci. Rev., 239, 106361, https://doi.org/10.1016/j.quascirev.2020.106361, 2020.

de Garidel-Thoron, T., Rosenthal, Y., Bassinot, F., Beaufort, L.: Stable Sea Surface Temperatures in the Western Pacific Warm Pool over the Past 1.75 Million Years, Nature, 433 (7023), 294–298. https://doi.org/10.1038/nature03189, 2005

de Garidel-Thoron, T., Rosenthal, Y., Beaufort, L., Bard, E., Sonzogni, C., Mix, A. C.: A Multiproxy Assessment of the Western Equatorial Pacific Hydrography during the Last 30 Kyr, Paleoceanogr., 22 (3). https://doi.org/10.1029/2006PA001269, 2007.

Heaton, T. J., Köhler, P., Butzin, M., Bard, E., Reimer, R. W., Austin, W. E. N., Ramsey, C. B., Grootes, P. M., Hughen, K. A., Kromer, B., Reimer, P. J., Adkins, J., Burke, A., Cook, M. S., Olsen, J., Skinner, L. C.: Marine20—The Marine Radiocarbon Age Calibration Curve (0–55,000 Cal BP), Radiocarbon, 62 (4), 779–820, https://doi.org/10.1017/RDC.2020.68, 2020.

Hobart, B., Lisiecki, L.E., Rand, D., Lee, T., Lawrence, C. E.: Late Pleistocene 100-kyr glacial cycles paced by precession forcing of summer insolation, Nat. Geosci., https://doi.org/10.1038/s41561-023-01235-x, 2023.

Holbourn, A., Kuhnt, W., Kawamura, H., Jian, Z., Grootes, P., Erlenkeuser, H., Xu, J.: Orbitally paced paleoproductivity variations in the Timor Sea and Indonesian Throughflow variability during the last 460 Kyr, Paleoceanogr., 20 (3), https://doi.org/10.1029/2004PA001094, 2005.

Hollstein, M., Mohtadi, M., Kienast, M., Rosenthal, Y., Groeneveld, J., Oppo, D. W., Southon, J. R., Lückge, A. The Impact of Astronomical Forcing on Surface and Thermocline Variability Within the Western Pacific Warm Pool Over the Past 160 Kyr, Paleoceanogr. and Paleoclimatol., 35 (6), e2019PA003832, https://doi.org/10.1029/2019PA003832, 2020.

Formatted: Font color: Text 1

Formatted: Font color: Text 1

Formatted: Font color: Text 1

Formatted: Font color: Text 1

Formatted: Font color: Text 1

Formatted: Font color: Text 1

Formatted: Font color: Text 1

Huybers, P., Wunsch, C.: A Depth-Derived Pleistocene Age Model: Uncertainty Estimates, Sedimentation Variability, and Nonlinear Climate Change, Paleoceanogr., 19 (1), https://doi.org/10.1029/2002PA000857, 2004.

Imbrie, J., Hays, J. D., Martinson, D. G., McIntyre A., Mix A. C., Morley, J. J., Pisias N. G., Prell, W. L., and Shackleton, N. J.: The orbital theory of Pleistocene climate: Support from a revised chronology of the marine $\delta^{18}O$ record, Milankovitch and Climate, Part 1, D. Reidel Publishing Company, Dordrecht, Netherlands, 269 pp., ISBN 9027717915, 1984.

Jian, Z., Wang, Y., Dang, H., Mohtadi, M., Rosenthal, Y., Lea, D. W., Liu, Z., Jin, H., Ye, L., Kuhnt, W., Wang, X.: Warm Pool Ocean Heat Content Regulates Ocean Continent Moisture Transport, Nature, 612 (7938), 92–99, https://doi.org/10.1038/s41586-022-05302-y, 2022.

Lee, T., Rand, D., Lisiecki, L. E., Gebbie, G., Lawrence, C. E.: Bayesian Age Models and Stacks: Combining Age Inferences from Radiocarbon and Benthic $\delta^{18}O$ Stratigraphic Alignment, EGUsphere, 1–29, https://doi.org/10.5194/egusphere-2022-734, 2022 (accepted for publications at Clim. Past)

Lea, D. W.: The 100,000-Yr Cycle in Tropical SST, Greenhouse Forcing, and Climate Sensitivity, American Meteorological Society: J. Clim., 17 (11), 2170–2179, https://doi.org/10.1175/1520-0442(2004)017<2170:TYCITS>2.0.CO;2, 2004.

Lea, D. W., Pak, D. K., Spero, H. J.: Climate Impact of Late Quaternary Equatorial Pacific Sea Surface Temperature Variations, Science, 289 (5485), 1719–1724, https://doi.org/10.1126/science.289.5485.1719, 2000.

Li L., Li, Q., Tian, J., Wang, P., Wang, H., Liu, Z.: A 4-Ma record of thermal evolution in the tropical western Pacific and its implications on climate change, Earth and Planet. Sci. Lett.,, 309, 10–20, doi.org/10.1016/j.epsl.2011.04.016, 2011.

Li, Z.; Shi, X., Chen, M. T.; Wang, H., Liu, S., Xu, J., Long, H., Troa, R. A., Zuraida, R., Triarso, E.: Late Quaternary Fingerprints of Precession and Sea Level Variation over the Past 35 Kyr as Revealed by Sea Surface Temperature and Upwelling Records from the Indian Ocean near Southernmost Sumatra, Quat. Int., 425, 282–291. https://doi.org/10.1016/j.quaint.2016.07.013, 2016.

Linsley, B. K., and M. T. von Breymann: Stable isotopic and geochemical record in the sulu sea during the last 750 k.y.:Assessment of surface water variability and paleoproductivity changes, Proceedings of the Ocean Drilling Program, Scientific Results, 24, 379-396, https://doi.org/10.2973/odp.proc.sr.124.151.1991,1991.

Linsley, B., Rosenthal, Y., Oppo, D.: Holocene Evolution of the Indonesian Throughflow and the Western Pacific Warm Pool, Nat. Geosci., 3, https://doi.org/10.1038/ngeo920, 2010.

Lisiecki, L. E., Raymo, M. E.: A Pliocene-Pleistocene Stack of 57 Globally Distributed Benthic $\delta^{18}O$ Records, Paleoceanogr., 20 (1), https://doi.org/10.1029/2004PA001071, 2005.

Lisiecki, L. E., Stern, J. V.: Regional and Global Benthic $\delta^{18}O$ Stacks for the Last Glacial Cycle, Paleoceanogr., 31 (10), 1368–1394, https://doi.org/10.1002/2016PA003002, 2016.

Lo, L., Chang, S. P., Wei, K. Y., Lee, S. Y., Ou, T. H., Chen, Y. C., Chuang, C. K., Mii, H. S., Burr, G. S., Chen, M. T., Tung, Y. H., Tsai, M. C., Hodell, D. A., Shen, C. C.: Nonlinear Climatic Sensitivity to Greenhouse Gases over Past 4 Glacial/Interglacial Cycles, Sci Rep, 7 (1), 4626, https://doi.org/10.1038/s41598-017-04031-x, 2017.

Locarnini, R. A., Mishonov, A. V., Baranova, O. K., Boyer, T. P., Zweng, M. M., Garcia, H. E., Reagan, J. R., Seidov, D., K. Weathers, Paver, C. R., and Smolyar, I.: Temperature, World Ocean Atlas 2018, NOAA Atlas NESDIS 81 [data set], https://archimer.ifremer.fr/doc/00651/76338/, 2019.

Oppo, D. W., Linsley, B. K., Rosenthal, Y., Dannenmann, S., Beaufort, L.: Orbital and Suborbital Climate Variability in the Sulu Sea, Western Tropical Pacific, Geochem., Geophys., Geosyst., 4 (1), 1–20, https://doi.org/10.1029/2001GC000260, 2003.

Regoli, F., de Garidel-Thoron, T., Tachikawa, K., Jian, Z., Ye, L., Droxler, A. W., Lenoir, G., Crucifix, M., Barbarin, N., Beaufort, L.: Progressive Shoaling of the Equatorial Pacific Thermocline over the Last Eight Glacial Periods, Paleoceanogr., 30 (5), 439–455, https://doi.org/10.1002/2014PA002696, 2015.

Rosenthal, Y., Oppo, D. W., Linsley, B. K.: The Amplitude and Phasing of Climate Change during the Last Deglaciation in the Sulu Sea, Western Equatorial Pacific, Geophys. Res. Lett., 30 (8). https://doi.org/10.1029/2002GL016612, 2003

Sadekov, A., Eggins, S. M., De Deckker, P., Ninnemann, U., Kuhnt, W., Bassinot, F.: Surface and Subsurface Seawater Temperature Reconstruction Using Mg/Ca Microanalysis of Planktonic Foraminifera Globigerinoides Ruber, Globigerinoides Sacculifer, and Pulleniatina Obliquiloculata, Paleoceanogr., 24 (3), https://doi.org/10.1029/2008PA001664, 2009.

Shakun, J. D., Lea, D. W., Lisiecki, L. E., Raymo, M. E.: An 800-Kyr Record of Global Surface Ocean δ δ^{18}O and Implications for Ice Volume-Temperature Coupling, Earth and Planet. Sci. Lett.,, 426, 58–68, https://doi.org/10.1016/j.epsl.2015.05.042, 2015.

Singer, B. S.: A Quaternary Geomagnetic Instability Time Scale, Quat. Geochronol., 21, 29–52, https://doi.org/10.1016/j.quageo.2013.10.003, 2014.

Spero, H. J., Mielke, K. M., Kalve, E. M., Lea, D. W., Pak, D. K.: Multispecies Approach to Reconstructing Eastern Equatorial Pacific Thermocline Hydrography during the Past 360 Kyr, Paleoceanogr., 18 (1), https://doi.org/10.1029/2002PA000814, 2003.

Spratt, R. M., Lisiecki, L. E. A Late Pleistocene Sea Level Stack, Clim. Past, 12 (4), 1079–1092, https://doi.org/10.5194/cp-12-1079-2016, 2016.

Tachikawa, K., Timmermann, A., Vidal, L., Sonzogni, C., Timm, O. E.: CO2 Radiative Forcing and Intertropical Convergence Zone Influences on Western Pacific Warm Pool Climate over the Past 400ka, Quat. Sci. Rev., 86, 24–34, https://doi.org/10.1016/j.quascirev.2013.12.018, 2014.

Visser, K., Thunell, R., and Stott, L.: Magnitude and Timing of Temperature Change in the Indo-Pacific Warm Pool during Deglaciation, Nature, 421, 152–155. https://doi.org/10.1038/nature01297, 2003.

Wang, L.: Isotopic Signals in Two Morphotypes of Globigerinoides Ruber (White) from the South China Sea: Implications for Monsoon Climate Change during the Last Glacial Cycle, Paleoceanogr., Palaeoclimatol., Palaeoecol., 161 (3), 381–394, https://doi.org/10.1016/S0031-0182(00)00094-8, 2000.

Xu, J., Holbourn, A., Kuhnt, W., Jian, Z., Kawamura, H.: Changes in the Thermocline Structure of the Indonesian Outflow during Terminations I and II, Earth and Planet. Sci. Lett., 273 (1), 152–162, https://doi.org/10.1016/j.epsl.2008.06.029, 2008.

Formatted: Normal, Space Before: 12 pt, After: 12 pt